

POLITECNICO DI MILANO

Dipartimento di Elettronica, Informazione e Bioingegneria



**REALIZATION OF AN EXTRACTED-POLE FILTER
IN COAXIAL TECHNIQUE**

Supervisor: Prof. Giuseppe Macchiarella

Name:

Mengze Cao 10652583

Jiaying Yang 10652576

Academic Year: 2020 - 2021

Table of Contents

List of Figures	3
List of Tables.....	6
1 introduction.....	7
2 Generality on Microwave Filters	9
2.1 Two-Port Networks	9
2.2 Classification of Filters	12
2.2.1 Classification by Amplitude-Frequency Characteristic.....	12
2.2.2 Classification by Structure and Technology	13
2.3 Normalized low-pass frequency domain	15
2.4 All-Pole Filter	17
2.5 Synthesis and Denormalization of Low-pass Prototype	18
2.6 Filter with Transmission Zeros	22
2.6.1 Cross-Coupled Filter	22
2.6.2 Extracted-Pole Filter.....	26
3 Design of Extracted-Pole Prototype Filters	30
3.1 Evaluation of Characteristic Polynomials	30
3.2 General Configuration of Extraction with NRN	33
3.3 Synthesis of the Low-Pass Prototype	36
3.4 De-normalization of the Low-Pass Prototype	40

4 Realization of an Extracted-Pole Filter in Coaxial Technology	46
4.1 Assignment of the Electrical Specification	46
4.2 Synthesis and De-normalization of a Low-Pass Prototype	51
4.3 Physical Implementation with Coaxial Technology	54
4.3.1 Global Variables.....	58
4.3.2 Local Variables.....	62
4.3.3 Cascading the Blocks with Suitable Lengths	69
5 Conclusion and Comments	74
Bibliography	78

List of Figures

2.1	The parameter of two-port networks	9
2.2	Type of filters by amplitude-frequency characteristic	12
2.3	Type of filters by amplitude-frequency characteristic	13
2.4	Type of filters by amplitude-frequency characteristic	13
2.5	Type of filters by amplitude-frequency characteristic	13
2.6	Synthesized filter of low-pass prototype	18
2.7	Low-pass prototype containing only series/shunt resonators	19
2.8	Equivalent circuits containing inverter of a de-normalized band-pass filter	21
2.9	A general process from requirements to a final physical microwave filter (all-pole filters)	22
2.10	Cross-coupling network	23
2.11	Conventional representation of a cross-coupled prototype network	24
2.12	Different kinds of canonical prototypes	25
2.13	Main blocks of cascaded-block technology	26
2.14	Box section technology	26
2.15	Cul-de-sac technology	27
2.16	Conventional representation of an extracted-pole prototype network	27
2.17	A general process of the design of an extracted-pole filter	29
3.1	Subsequent extraction of the circuit elements from the [ABCD] matrix	34
3.2	frequency-invariant susceptance with value B_{nrrn}	34

3.3	General configuration of extraction with NRN	35
3.4	Transformation from wheel prototype to inline extracted-pole topology	37
3.5	Obtained triplet from n-x matrix rotation	38
3.6	D2S transformation	38
3.7	Synthesized equivalent circuit of the extracted pole filter	39
3.8	De-normalized filter with all the inverters equal to K_0 except the central one	40
3.9	B_k as resonant nodes and B_k as non-resonant nodes	41
3.10	Transformation of the impedance inverter with $J > J_0$	42
3.11	Configuration of the PZP block (shunt model)	43
3.12	De-normalized filter with all the resonators assigned	44
4.1	Synthesized bandpass filter	47
4.2	Equivalent circuit of a synthesized bandpass filter	48
4.3	Synthesized bandpass filter with 2 reflection zeros	48
4.4	Obtained final results of scattering parameters	51
4.5	Routing scheme of the synthesized filter	52
4.6	Equivalent circuit of the filter with assigned inverters	52
4.7	Transformation of the admittance inverter to the phase shifter	53
4.8	Final scheme of the synthesized filter	54
4.9	Computed frequency response	54
4.10	Physical model of the PZP block	55
4.11	Shunt equivalent circuits	56
4.12	Dimension parameters of the model of PZP block	57
4.13	Dimension parameters of the model of PZP block	57
4.14	Relationship between s , Rs and Z_0	59
4.15	Relationship between H_z and f_z	59
4.16	Relationship between D and f_z	60
4.17	Relationship between gap and f_z	60
4.18	Relationship between $blank$ and f_z	60
4.19	Relationship between $Wstrip$ and f_z	61
4.20	X_{eq} vs. Rs for different values of s	63

4.21 X_{eq} vs. s for different values of R_s	63
4.22 B_{nrn} vs. R_s for different values of s	64
4.23 B_{nrn} vs. s for different values of R_s	64
4.24 s vs. R_s for block 1	65
4.25 s vs. R_s for block 2	65
4.26 s vs. R_s for block 3	66
4.27 s vs. R_s for block 4	66
4.28 Scattering parameters of block 1	67
4.29 Scattering parameters of block 2	67
4.30 Scattering parameters of block 3	67
4.31 Scattering parameters of block 4	68
4.32 Final Equivalent Circuit of Cascade-Blocks	69
4.33 Wavelength calculator	70
4.34 Physical model of the final filter	71
4.35 Retouch of the connection length in the circuit simulator AWR	71
4.36 Scattering parameters of the filter in the circuit simulator AWR	72
4.37 Structure of the final filter	72
4.38 Scattering parameters of the final filter	73
5.1 $X_{eq} = 48.522$, $B_{nrn} = -1.4$	75
5.2 Physical implementation of PZP block with addition short-circuited post	76

List of Tables

2.1 Transformation of components at circuits level	21
4.1 Geometrical dimension variables in the design of PZP block	58
4.2 Assignment of global parameters	62
4.3 Required (X_{eq}, B_{nrn}) for each block	65
4.4 (Rs, s) solution pairs for each block	66
4.5 Comparison of X_{eq}, B_{nrn} of synthesized result, before tuning and after tuning	68
4.6 lengths ϕ_p of the equivalent circuit of the dimensioned blocks	69
4.7 Computed lengths from the synthesized result	69
4.8 Transformation from electrical lengths to physical lengths	70
4.9 Distances between blocks	71
4.10 Final computed distances $d_{i,i+1}$	71

Chapter 1

Introduction

In recent years, with the rapid development of microwave technologies, wireless communication systems have developed vigorously. As a frequency selection device, microwave filter is a very important part of modern microwave communication systems. The performance of microwave filters directly affects the entire communication systems. As the electromagnetic environment becomes more and more complex and frequency congestion becomes more and more serious, higher and stricter requirements are set for microwave filters. Therefore, how to design a filter with high stopband suppression, wide frequency band, in-band flatness and narrow transition band has become a topic of concern.

Microwave filters can be generally divided into two kind: all-pole filters and filters with transmission zeros. All-pole filters include Butterworth filter, Chebyshev filter, ellipse filter, etc. Filters with transmission zeros mainly include cross-coupling filters and extracted-pole filters.

Extracted-pole filters are widely used nowadays for several reasons. Firstly, as a filter with transmission zeros, an extracted-pole filter can introduce transmission zeros in the stop band, which could lead to a steep out-of-band suppression and a narrow transition band. Secondly, compared with cross-coupling filters, extracted-pole filters become especially good when we need many transmission zeros. It is because that when the number of transmission

zeros is large, a cross-coupling filter will have problem with geometrical control, complex layout and spurious coupling. Thirdly, it is important that an extracted-pole filter has an inline (quasi-inline) configuration, which has opposite input and output, reducing the direct feedthrough and making it easy to realize channel filters in combiners and multiplexers.

In conclusion, the thesis will introduce a design approach of extracted-pole filters based on coaxial technology. It is then divided as follows:

In chapter 2, the general concepts of microwave filters are introduced, including the definition and main parameters of a microwave filter, classifications of filters by different means, all-pole filters and filters with transmission zeros from the initial technical specification.01

In chapter 3, firstly the Chebyshev transfer function polynomials approximation is introduced. Then details about the synthesized extracted-pole prototype filters are shown, including general configuration, basic components, transformation algorithm. Finally the de-normalization procedure is introduced step by step, until we get the equivalent circuit suitable for physical implementation.

In chapter 4, we will discuss all the steps taken in order to realize an extracted-pole band-stop filter in a coaxial cavity structure, from the initial requirements to the geometrical dimension of final physical filter. A general method of geometrical dimension is introduced particularly.

In chapter 5, the discussion of the results obtained is reported.

Chapter 2

Generality on Microwave Filters

In this chapter, we will discuss the general concepts of microwave filters, including necessary basics of filters, different kinds of microwave filters, structure and design of all-pole filters and filters with transmission zeros.

2.1 Two-Port Networks

A microwave circuit can be represented as a network. Considering a microwave filter, it can be considered as a 2-port junction network, which operates on signals in the gigahertz frequency ranges [1], as shown in Fig.2.1.

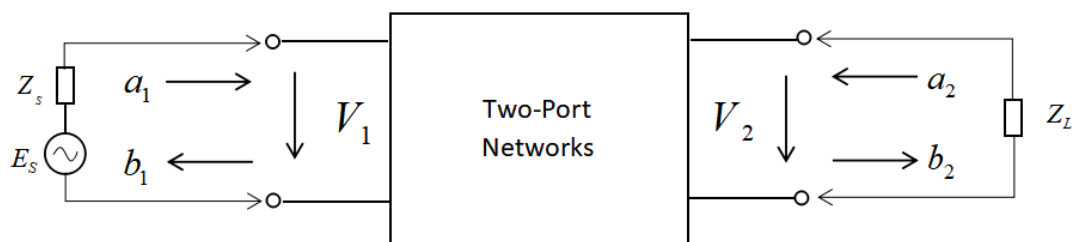


Figure 2.1: The parameter of two-port networks

2.1 Two-Port Networks

To analyse microwave circuits, the most commonly used parameter matrices are $[Z]$ impedance matrix, $[Y]$ admittance matrix, $[S]$ scattering matrix, and $[T]$ transmission matrix. Actually, though these four kinds of parameter matrix are defined by different physical meanings, they can be transformed into each other. We discuss mainly $[Z]$ impedance matrix and $[S]$ scattering matrix of a two-port network in the following.

Referring to the figure of two-port network above, we can describe the relationship between voltage and current through $[Z]$ impedance matrix:

$$\begin{bmatrix} V_1 \\ V_2 \end{bmatrix} = \begin{bmatrix} Z_{11} & Z_{12} \\ Z_{21} & Z_{22} \end{bmatrix} \begin{bmatrix} I_1 \\ I_2 \end{bmatrix} \quad (2.1)$$

The corresponding physical meaning are:

$$Z_{11} = \left. \frac{V_1}{I_1} \right|_{I_2=0} \quad Z_{12} = \left. \frac{V_1}{I_2} \right|_{I_1=0} \quad Z_{21} = \left. \frac{V_2}{I_1} \right|_{I_2=0} \quad Z_{22} = \left. \frac{V_2}{I_2} \right|_{I_1=0} \quad (2.2)$$

scattering matrix describes the relationship between incident and reflected normalized voltage/current waves at two ports. Considering the 2-port network in the figure above, we have:

$$\begin{bmatrix} V_1^- \\ V_2^- \end{bmatrix} = \begin{bmatrix} S_{11} & S_{12} \\ S_{21} & S_{22} \end{bmatrix} \begin{bmatrix} V_1^+ \\ V_2^+ \end{bmatrix} \quad (2.3)$$

The corresponding physical meaning are

2.1 Two-Port Networks

$$S_{11} = \left. \frac{V_1^-}{V_1^+} \right|_{V_2^+=0} \quad S_{22} = \left. \frac{V_2^-}{V_2^+} \right|_{V_1^+=0} \quad S_{12} = \left. \frac{V_1^-}{V_2^+} \right|_{V_1^+=0} \quad S_{21} = \left. \frac{V_2^-}{V_1^+} \right|_{V_2^+=0} \quad (2.4)$$

[S] scattering matrix is the most commonly used matrix in the design of microwave filter since it is easy to measure from network. What's more, when we have already got [S] scattering matrix, it is convenient to compute the other parameter matrix from [S].

The main technical parameters for the design of filter are listed as following:

Return loss: Return loss is defined as the ratio of the reflected wave power to the incident wave power at the port of the transmission line. For simplicity, return loss is often expressed as a ratio in decibels(*dB*)

$$RL(dB) = 10 \log_{10} \frac{P_i}{P_r} = 10 \log_{10} |S_{11}|^2 \quad (2.5)$$

Insertion loss: Insertion loss is defined as the loss due to the insertion of a device into a transmission line. For simplicity, insertion loss is often expressed as a ratio in decibels (*dB*).

$$IL(dB) = 10 \log_{10} \frac{P_T}{P_R} = 10 \log_{10} |S_{21}|^2 \quad (2.6)$$

Bandwidth: It is usually defined as the difference between upper and lower frequency within a passband (or stopband).

Quality factor: It is usually defined as the ratio of the energy stored in the resonator to the energy dissipated per cycle.

Group delay: We define group delay to quantify the requirements on the phase linearity. Group delay is the deviation from the linear phase dependence, it is defined with ϕ phase of S_{21} :

2.2 Classification of Filters

$$\tau_{GD} = -\frac{d\phi(\omega)}{d\omega} \quad (2.7)$$

Then we can translate the specification of phase linearity in requiring a maximum percentage variation of group delay within the band.

Central frequency: It is usually defined as the midpoint between two 3dB points of a band-pass filter (or band-stop filter) and is usually represented by the arithmetic average of the two 3dB points.

2.2 Classification of Filters

There are different ways to classify microwave filters, for example, classification by structure, classification by the width of passbands, classification by operation ways.

2.2.1 Classification by Amplitude-Frequency Characteristic

Considering amplitude-frequency characteristic, we can classify microwave filters into four general categories which are shown in the following:

- Low-pass filter: allows signal below cut-off frequency pass, otherwise large signal attenuation exists, as shown in Fig.2.2.
- High-pass filter: allows signal above cut-off frequency pass, otherwise large signal attenuation exists, as shown in Fig.2.3.
- Band-pass filter: allows signal in a specific band pass, otherwise large signal attenuation exists, as shown in Fig.2.4.
- Band-stop filter: allows signal except a specific band pass, while large signal attenuation exists in this specific band, as shown in Fig.2.5.

2.2 Classification of Filters

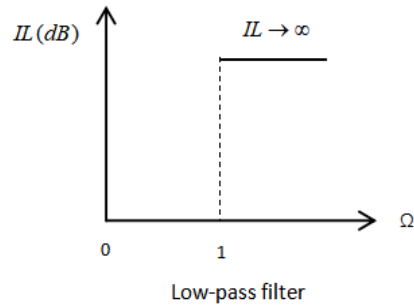


Figure 2.2: Type of filters by amplitude-frequency characteristic

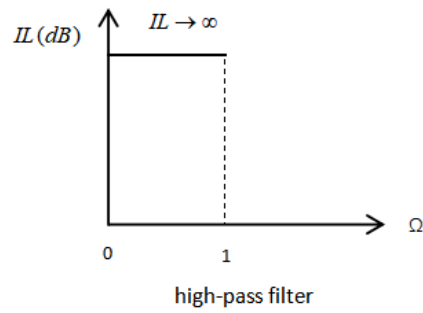


Figure 2.3: Type of filters by amplitude-frequency characteristic

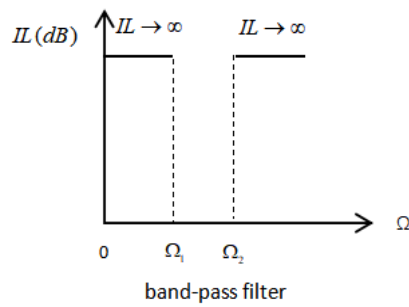


Figure 2.4: Type of filters by amplitude-frequency characteristic

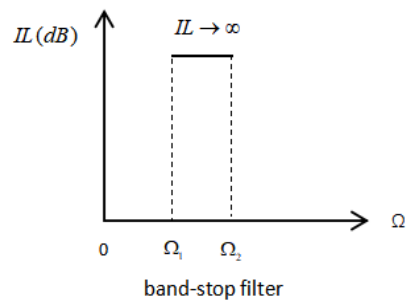


Figure 2.5: Type of filters by amplitude-frequency characteristic

2.2.2 Classification by Structure and Technology

Considering filter structures and technology, several kinds of microwave filters are shown in the following

(1) Lumped-element LC filter

When the physical dimension of a circuit network is much smaller than the electrical wavelength of signal, which means the signal frequency is not too large, a lumped-element LC filter can be used. To be more specific when the signal frequency is larger than 1GHz, which means the physical dimension is comparable with electrical wavelength, distribution parameter effect will significantly decrease the performance of the filter.

(2) Planar filter

Planar filters are created with flat 2D resonators with pattern of strip on a dielectric substrate. Considering different transmission lines to make resonators, there are different kinds of planar filters, such as stripline, microstrip and coplanar waveguide. Planar filters have operating frequency among MHz to GHz, and Q factor is related with filter materials.

(3) MEMS (Micro-Electro-Mechanical System) filter

MEMS filter is a microwave filter manufactured based on MEMS technology. MEMS technology can realize the integration of microwave passive devices without sacrificing device performance. Microwave filters based on MEMS technology not only have excellent frequency selection ability and low insertion loss, but also have much smaller size than traditional microwave filters.

(4) Cavity filter

A cavity filter is a filter based on resonant cavity, which can be considered as a capacitor in parallel with an inductor. There are several kinds of cavity filters due to their different structures and materials.

2.2 Classification of Filters

- Coaxial cavity filter

Coaxial cavity filters are widely used since they have advantages of high Q value, good electromagnetic shielding, low loss and small size. The design of a coaxial cavity filter has large freedom. For example, the structure of resonant cavity could be either round or square. Also coaxial cavity filters can easily achieve cross-coupling between non-adjacent cavities to get multiple asymmetrical out-of-band attenuation poles.

- Waveguide filter

Waveguides are hollow metal conduits, in which electromagnetic waves can be transmitted. The resonant cavities in waveguide filters are based on a short length of waveguide blocked at both ends. Waveguide filters have high Q values, low insertion loss, and they are easy to be manufactured. However, as a kind of transmission line filters, waveguide filters have multiple passbands due to the intrinsic property of transmission line filters, but usually only the lowest frequency passband is useful, and the other passband may damage the performance of the filter.

- Comb filter

In a comb filter, the resonators are made of capacitive load metal rods of various wavelengths. The comb filter is usually implemented by a Chebyshev function. Its main characteristics are small size, low loss, moderate Q value, and the parasitic passbands are usually far away from the lowest passband.

- Helical filter

Helical filters are based on helical resonators, which is similar to $1/4$ wavelength coaxial line resonator. The spiral resonator is actually a special kind of coaxial cavity. The difference between them is that the inner conductor of helical resonator is a spiral, while the one of the coaxial cavities is straight. The main characteristics of helical filters are small size, high Q value, and they are easy to be manufactured.

2.3 Normalized Low-pass Frequency Domain

Actually, we perform the synthesis of filter in a normalized low-pass domain, which is defined by frequency transformations. Then we can de-normalize the circuit synthesized in the low-pass domain through appropriate circuit transformation. Consequently, we should firstly transform the specification of filters in the initial frequency domain to that in the normalized low-pass domain.

We define Ω as the frequency variable in the normalized low-pass domain, ω as the frequency variable in the initial frequency domain, the frequency transformation of four basic filters is reported as follows:

- Low-pass filter

$$\Omega = \frac{\omega}{\omega_c} \quad (2.8)$$

- High-pass filter:

$$\Omega = \frac{\omega_c}{\omega} \quad (2.9)$$

- Band-pass filter:

$$\Omega = \frac{\omega_0}{\Delta\omega} \left(\frac{\omega}{\omega_0} - \frac{\omega_0}{\omega} \right) \quad (2.10)$$

- Band-stop filter:

$$\Omega = \frac{1}{\frac{\omega_0}{\Delta\omega} \left(\frac{\omega}{\omega_0} - \frac{\omega_0}{\omega} \right)} \quad (2.11)$$

Where ω_c represents unnormalized cut-off frequency, $\omega_0 = \sqrt{\omega_1\omega_2}$ represents band centre frequency, $\Delta\omega = \omega_2 - \omega_1$ represents passband/stopband bandwidths.

With the frequency transformation equation above, we can easily derive the frequency characteristics in the normalized low-pass domain. The next step is to choose an approximant function that satisfying the frequency characteristics in the normalized low-pass domain.

2.4 All-Pole Filter

$$A(\Omega) = 1 + \varepsilon^2 C_n^2(\Omega) \quad (2.12)$$

Where $A(\Omega)$ is attenuation in the normalized low-pass domain, ε defines the maximum losses ($\Omega = \pm 1, |C_n| = 1, A_{max} = 1 + \varepsilon^2$), C_n is characteristic function of filter that defines the approximation of ideal filter response (specification).

With $s = j\Omega$, $C_n(s)$ can be expressed as the ratio of two polynomials:

$$C_n(s) = \frac{F(s)}{P(s)} \quad (2.13)$$

The roots of $F(s)$ are called reflection zeros, deriving $A = 1$. The roots of $P(s)$ are called transmission zeros. When $P(s) = \text{constant}$, which means there is no transmission zeros, we call them all-pole filters.

2.4 All-Pole Filter

(1) Butterworth filter

Butterworth filter is also called maximally flat filter. It is due to that Butterworth filter requires the maximum flatness in the passband with no ripple. The characteristic function is defined as:

$$C_n(\Omega) = \Omega^n \quad (2.14)$$

(2) Chebyshev filter

Chebyshev filter is a filter with equal ripple fluctuations in the passband. The characteristic function is defined as:

2.5 Synthesis and De-normalization of Low-Pass Prototype

$$C_n(\Omega) = \begin{cases} \cos(n \cdot \cos^{-1}(\Omega)) & |\Omega| \leq 1 \\ \cosh(n \cdot \cosh^{-1}(\Omega)) & |\Omega| > 1 \end{cases} \quad (2.15)$$

With $|C_n(\pm 1)|^2 = 1$.

As shown above, the order of filter is needed to be determined, which is related with the filter specification.

$$n \geq \frac{A_M + RL}{20 \log(\Omega_s)} \quad \text{Butterworth characteristic} \quad (2.16)$$

$$n \geq \frac{A_M + RL + 6}{20 \log(\Omega_s) + 6} \quad \text{Chebycheff characteristic} \quad (2.17)$$

where RL is passband return loss, A_M is stopband minimum attenuation, Ω_s is cut-off frequency in the normalized low-pass domain.

2.5 Synthesis and De-normalization of Low-Pass Prototype

Prototype

After determining the type and order of low-pass prototype, we can easily derive the corresponding characteristic function. Then we can perform the synthesis of low-pass prototype, as shown in Fig.2.6.

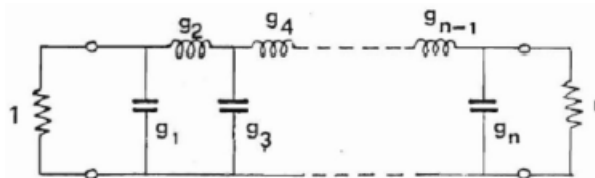


Figure 2.6: Synthesized filter of low-pass prototype

2.5 Synthesis and De-normalization of Low-Pass Prototype

For Butterworth filter, we have:

$$r_n = 1 \quad (2.18)$$

$$g_q = 2a_q \sqrt[n]{\varepsilon} \quad (2.19)$$

$$a_q = \sin\left(\frac{(2q-1)\pi}{2n}\right) \quad (2.20)$$

For Chebyshev filter, we have:

$$r_n = 1 \quad (n \text{ odd}) \quad (2.21)$$

$$r_n = [\sqrt{1 + \varepsilon^2} - \varepsilon]^2 \quad (n \text{ even}) \quad (2.22)$$

$$g_1 = \frac{2a_1}{\gamma} \quad (2.23)$$

$$g_q = \frac{4a_{q-1} \cdot a_q}{b_{q-1} \cdot g_{q-1}} \quad (2.24)$$

$$a_q = \sin\left(\frac{(2q-1)\pi}{2n}\right) \quad (2.25)$$

$$\gamma = \sinh\left(\frac{1}{2n} \ln\left(\frac{\sqrt{1+\varepsilon^2}+1}{\sqrt{1+\varepsilon^2}-1}\right)\right) \quad (2.26)$$

$$b_q = \gamma^2 + \sin^2\left(\frac{q\pi}{n}\right) \quad (2.27)$$

Compared to Butterworth filters, Chebyshev filters are sharper and have better selectivity index. With the same filter order, the most important advantage is that Chebyshev filters minimize the error between the ideal and the actual filter characteristic over the range of the filter. Then we choose Chebyshev filters in the following analysis.

2.5 Synthesis and De-normalization of Low-Pass Prototype

It is necessary to have only series or shunt resonators and it is obtained by the introduction of impedance(admittance) inverters. The two models (which actually are equivalent) are successively shown in Fig.2.7:

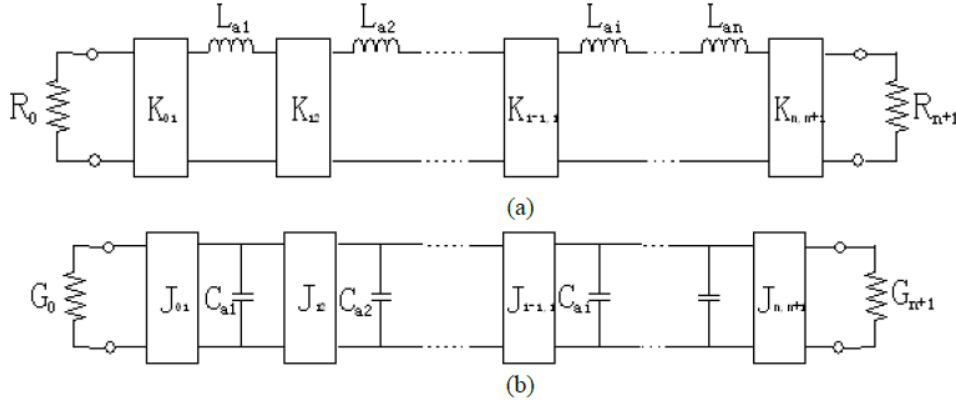


Figure 2.7: Low-pass prototype containing only series/shunt resonators

In figure (a), it contains only impedance inverters and series inductance.

$$K_{0,1} = \sqrt{\frac{R_0 L_{a1}}{g_0 g_1}}, K_{i,i+1} = \sqrt{\frac{L_{ai} L_{a,i+1}}{g_i g_{i+1}}} (i = 1 \dots n - 1), K_{n,n+1} = \sqrt{\frac{L_{an} R_{n+1}}{g_n g_{n+1}}} \quad (2.28)$$

In figure (b), it contains only admittance inverters and shunt capacitance.

$$J_{0,1} = \sqrt{\frac{G_0 C_{a1}}{g_0 g_1}}, J_{i,i+1} = \sqrt{\frac{C_{ai} C_{a,i+1}}{g_i g_{i+1}}} (i = 1 \dots n - 1), J_{n,n+1} = \sqrt{\frac{C_{an} G_{n+1}}{g_n g_{n+1}}} \quad (2.29)$$

What's more, the introduction of inverters brings an increase in degrees of freedom (inverters or resonators parameter). There are usually two particular solutions.

2.5 Synthesis and De-normalization of Low-Pass Prototype

All inverter parameters are the same value, then all resonators parameters are different from each other.

All resonator parameters are the same value, then all inverters parameters are different from each other.

The next step is de-normalization of the low-pass prototype shown above. At circuit level, we can transform the components (capacitor, inductor) in the normalized low-pass prototype into the components in the de-normalized frequency domain, as shown in Tab.2.1.











Normalized	De-normalized			
Low-pass	Low-pass	High-pass	Band-pass	Band-stop
 $L = g_k$	 $\frac{L}{\omega_c}$	 $\frac{1}{\omega_c L}$	 $\frac{L}{BW}$	 $\frac{1}{BWL}$
 $C = g_k$	 $\frac{C}{\omega_c}$	 $\frac{1}{\omega_c C}$	 $\frac{C}{BW}$	 $\frac{1}{BWC}$

Table 2.1: Transformation of components at circuits level

Until now we have got the equivalent circuit suitable for implementation. In Fig.2.8 we take a band-pass filter as an example.

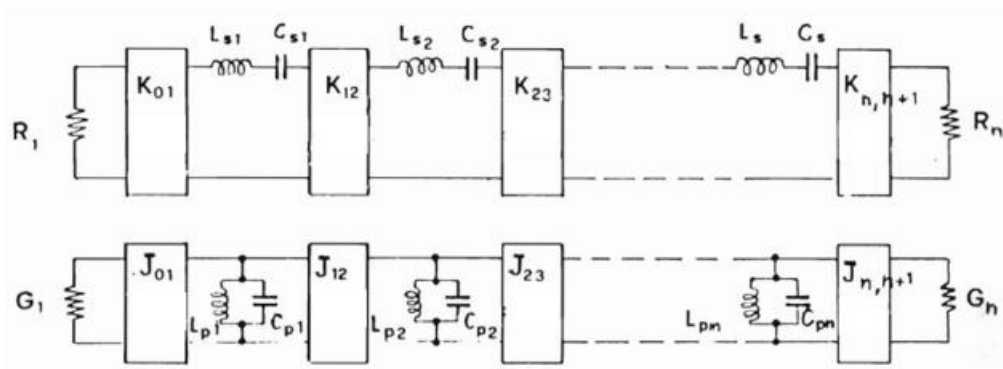


Figure 2.8: Equivalent circuits containing inverter of a de-normalized band-pass filter

2.6 Filters with Transmission Zeros

The last step is to choose a suitable implementation technology and translate the equivalent circuit into a physical filter.

For more clarity, a flow chart about a general process from requirements to a final physical microwave filter is shown in Fig.2.9.

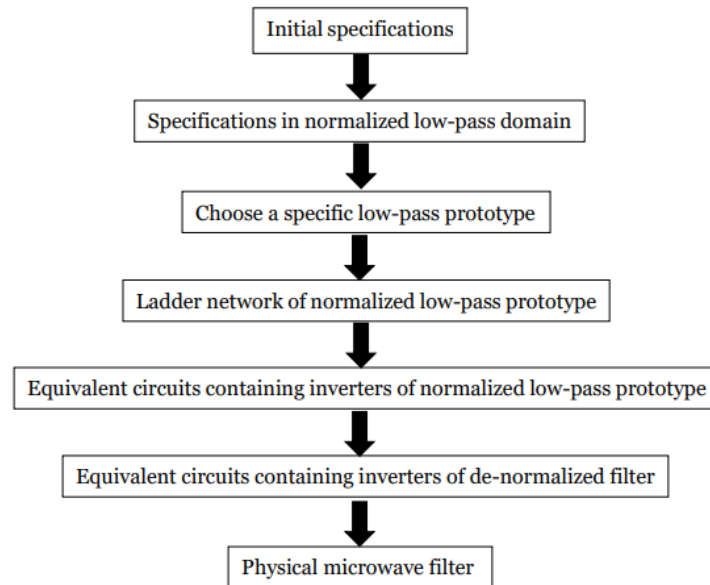


Figure 2.9: A general process from requirements to a final physical microwave filter (all-pole filters)

2.6 Filters with Transmission Zeros

When we need to satisfy very strict requirements, we have two choices. The first choice is to increase the filter order, but it will increase the number of resonators at the same time. Consequently, this choice will increase the filter volume, and insertion loss, which damages the filter performance.

The second choice is to introduce transmission zeros in the stop band, in proximity of the passband. These transmission zeros will increase the slope of the in-band attenuation curve and reduce the transition domain, which allow engineers to satisfy strict requirements with lower filter order.

2.6 Filters with Transmission Zeros

However, Butterworth and Chebyshev filters characteristics do not exhibit transmission zeros. So we introduce two kinds of filter called cross-coupled filter and extracted-pole filter. They allow the introduction of transmission zeros in the stop band.

What's more, we cannot apply the synthesis method of all-pole filters directly in this kind of filters. The reason is that the synthesis method of all-pole filters is based on the symmetry in the bandpass domain, while filters with transmission zeros presents an asymmetric response. Consequently, a new synthesis method is needed.

2.6.1 Cross-Coupled Filter

It is called cross-coupled filter because this kind of filter introduces transmission zeros through suitable coupling between non-adjacent nodes, which allows the signal of particular frequencies to reach the output nodes, as shown in Fig.2.10.

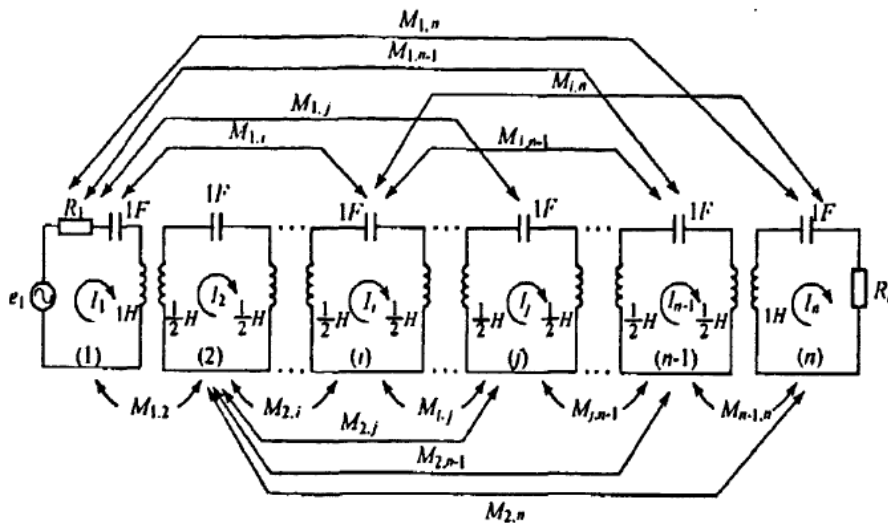


Figure 2.10: Cross-coupling network

For simplicity, we can represent a cross-coupled filter with “nodes” and “lines”. A node represents a capacitor in parallel with a frequency-invariant susceptance. A line represents an admittance inverter. In Fig.2.11 an example is shown.

2.6 Filters with Transmission Zeros

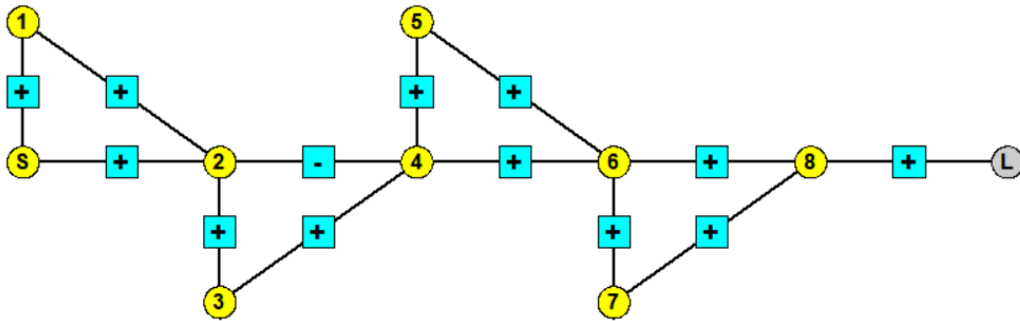


Figure 2.11: Conventional representation of a cross-coupled prototype network

To determine the maximum number of transmission zeros, it is necessary to introduce a concept called “minimum path rule”: The maximum number of transmission zeros (nz) is equal to the prototype order (n) minus the number of nodes touched for going from the source to the load (np).

$$nz = n - np \quad (2.30)$$

In the example shown above, $n=8$, $np=4$, so $nz=4$. The maximum number of transmission zeros is 4.

To satisfy a very strict requirement or get a good performance, we can increase the number of introduced transmission zeros. The maximum number is equal to the number of poles, which is also the filter order. When it happens, we call this kind of filter “fully canonical filter”.

In Fig.2.12 the most important canonical prototypes.

2.6 Filters with Transmission Zeros

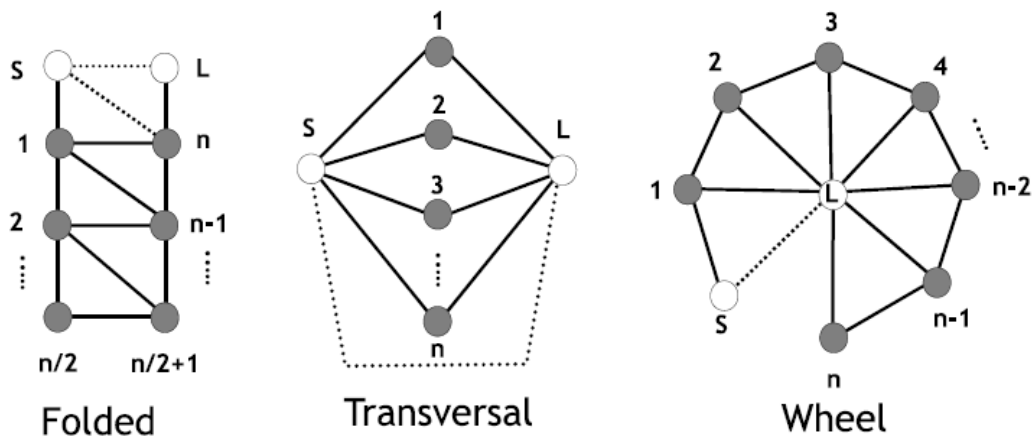


Figure 2.12: Different kinds of canonical prototypes

It is worth to mention that not all the couplings are different from zero except transversal prototype. As shown in the figure above, there are two kinds of couplings: the ones connecting sequential nodes called direct-couplings, and the ones connecting not-consecutive nodes called cross-couplings.

Concerning the synthesis of canonical prototypes, we can perform direct synthesis of canonical prototypes with the help of coupling matrix. Coupling matrix can also help us transform one kind of canonical prototype to another.

However, canonical prototypes are not used in the practice due to several reasons. One important reason is that there are too many couplings from load or source and there are too many couplings affecting transmission zeros.

Actually, we can refer to non-canonical prototypes. There are different kinds of non-canonical prototypes, for example, cascaded-block, box section, cul-de-sac, etc.

For cascaded-block technology, the main blocks shown in Fig.2.13 are the triplet (extracting 1 transmission zero) and quadruplet (extracting 2 transmission zeros). When cascading the blocks, we should pay attention that each block can only share one node.

2.6 Filters with Transmission Zeros

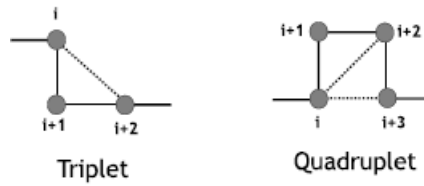


Figure 2.13: Main blocks of cascaded-block technology

The maximum number of transmission zeros allowed by cascaded-technology depends on whether source and load are used for cross-coupling.

Source and load are not used for cross-coupling

$$nz_{max} = \frac{n}{2} (n \text{ even}), nz_{max} = \frac{n-1}{2} (n \text{ odd}) \quad (2.31)$$

Source and load are used for cross-coupling.

$$nz_{max} = \frac{n+2}{2} (n \text{ even}), nz_{max} = \frac{n+1}{2} (n \text{ odd}) \quad (2.32)$$

For box section configuration shown in Fig.2.14, the maximum number of allowed transmission zeros is $(n - 2)/2$.

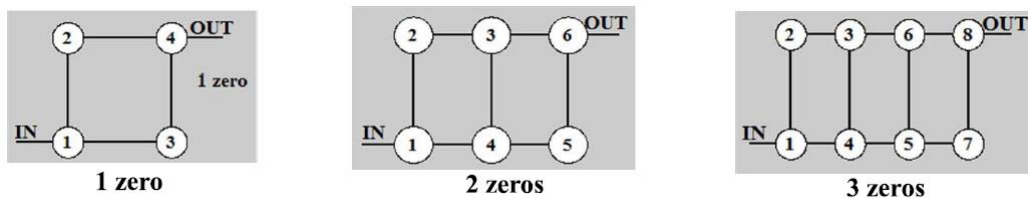


Figure 2.14: Box section technology

2.6 Filters with Transmission Zeros

For cul-de-sac configuration shown in Fig.2.15, the maximum number of allowed transmission zeros is $(n - 3)$.

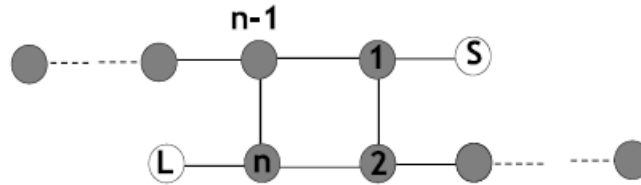


Figure 2.15: Cul-de-sac technology

2.6.2 Extracted-Pole Filter

This technology becomes especially good when we need many transmission zeros. For cross-coupled filters, when we need many transmission zeros (larger than half of order), each transmission zero will be affected by many other couplings, which is hard to control.

It is worth to mention that extracted-pole filter is a essentially in-inline topology. With an inline topology, input and output is opposite, then we can reduce the direct feedthrough and make it easy to realize channel filters in combiners and multiplexers.

Extracted-pole filters realize transmission zeros through the use of non-resonant nodes connecting with resonators. Each pair of a non-resonator node and a resonator will realize a transmission zero, as shown in Fig.2.16.

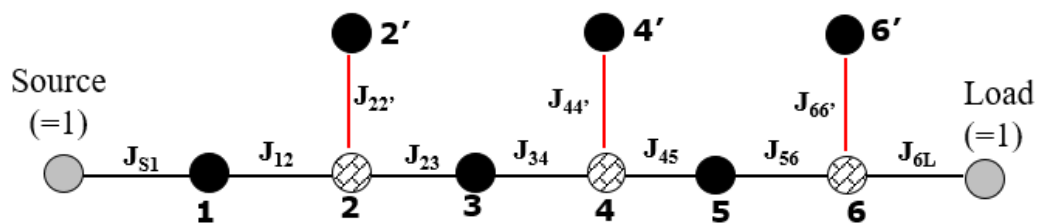


Figure 2.16: Conventional representation of an extracted-pole prototype network

2.6 Filters with Transmission Zeros

The black one is a resonator, another is NRN, and the line represents an inverter. In the figure shown above, there are obviously three transmission zeros.

NRN is frequency-invariant reactance (susceptance). On one hand, it brings convenience because the synthesis of filters with NRN can be performed in low pass domain and de-normalization will not change the values of NRNs. Then we can directly perform synthesis method on lowpass prototype.

On the other hand, since the coupling between NRNs cannot be related to the eigenmodes of the coupled physical structure, the existence of NRN makes the coupling matrix not meaningful. Consequently, the synthesized method through reconfiguration of coupling matrix cannot be used. We need to use some typical synthesized methods.

The number of synthesized equivalent circuits could be infinite, which is intrinsically redundant. But the filter response is determined by a set of universal parameters whose number is lower than the circuits variables. Generalized coupling coefficients (GCC) represents these universal parameters [2]:

$$k_{i,j} = \frac{J_{i,j}}{\sqrt{B_i \cdot B_j}}, \quad k_{S1} = \frac{J_{S1}^2}{B_1}, \quad k_{NL} = \frac{J_{NL}^2}{B_N} \quad (2.33)$$

Where

$$B_i = \begin{cases} |B_{NR,i}| & (\text{Nonresonant susceptance}) \\ B_{eq,i} & (\text{Resonant susceptance}) \end{cases} \quad (2.34)$$

It is worth mentioning that $B_{eq,i}$ is defined as usual. i.e.

$$B_{eq,i} = (1/2)(\partial B_{ris,i} / \partial \omega) \Big|_{\omega=\omega_0} \quad (2.35)$$

$B_{ris,i}(\omega)$ represents the total susceptance of the i-th resonator.

2.6 Filters with Transmission Zeros

GCC links the synthesized equivalent circuit with the geometric dimensions of the physical structure.

So far, we have a general approach to design an extracted-pole filter with non-resonating nodes. The flow chart is shown in Fig.2.17:

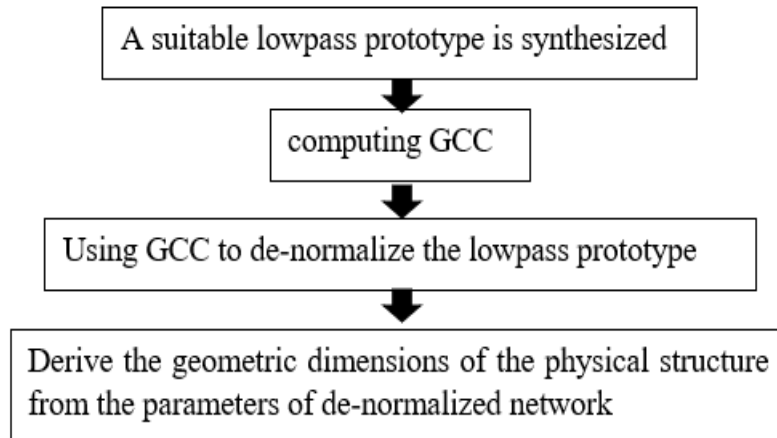


Figure 2.17: A general process of the design of an extracted-pole filter

Chapter 3

Design of extracted-pole prototype filters

In this chapter, firstly the evaluation of characteristic polynomials is discussed. Then details about the synthesized extracted-pole prototype filters are introduced, including general configuration, basic components, transformation algorithm. Finally the denormalization procedure is introduced step by step, until we get the equivalent circuit suitable for physical implementation.

3.1 Evaluation of Characteristic Polynomials

To start the design of filter, we use generalized Chebyshev function to have equal ripple. Actually when the filter order and transmission zeros are determined (for a bandpass filter), the response of a generalized Chebyshev filter is determined. For a bandstop filter, filter order and reflection zeros will determine the filter response (which will be discussed in chapter 4, here we take bandpass filter as an example). Consequently

3.1 Evaluation of Characteristic Polynomials

the first step is to derive the filter order and transmission zeros from the initial requirements in the normalized low pass domain. Then with the filter order and required transmission zeros suitably assigned, we can compute the characteristic polynomials of the normalized low-pass prototype. This step is called “synthesis of characteristic polynomials”. The detailed algorithm is introduced in the literature [6]. Here we will make a brief introduction to the general concept.

The generalized Chebyshev characteristic function is:

$$C_n(\Omega) = \begin{cases} \cos \left[(n - n_z) \cos^{-1}(\Omega) + \sum_k^{1, n_z} \left| \operatorname{Re} \left\{ \cos^{-1} \left(\frac{1 - \Omega \cdot \Omega_{z,k}}{\Omega - \Omega_{z,k}} \right) \right\} \right| \right] & |\Omega| \leq 1 \\ \cosh \left[(n - n_z) \cosh^{-1}(\Omega) + \sum_k^{1, n_z} \left| \operatorname{Re} \left\{ \cosh^{-1} \left(\frac{1 - \Omega \cdot \Omega_{z,k}}{\Omega - \Omega_{z,k}} \right) \right\} \right| \right] & |\Omega| > 1 \end{cases} \quad (3.1)$$

$\Omega_{z,k}$ are the assigned transmission zeros.

For a bandpass filter, firstly we assign the filter order n and number and location of transmission zeros. Then we could get the generalized Chebyshev filtering function $C_n(\Omega)$. Given $C_n(\Omega)$, we can now perform the evaluation of the characteristic polynomials:

$$C_n(s) = \frac{\varepsilon F(s)}{\varepsilon' P(s)} \quad (3.2)$$

Where the constant ε' is computed by RL:

$$|\varepsilon'|^2 = \frac{10^{-RL/10}}{1 - 10^{-RL/10}} \quad (3.3)$$

Assuming the polynomials $P(s)$ and $F(s)$ monic (max degree coefficient equal to one), the constant ε is given by:

3.1 Evaluation of Characteristic Polynomials

$$\varepsilon = \varepsilon' |P(\pm j)/F(\pm j)| \quad (3.4)$$

Since $zP_k = j\Omega_{z,k}$, zP_k are the roots of $P(s)$, which must be imaginary or complex pairs with opposite real part. Then $C_n(\Omega)$ can be expressed in terms of the roots of $P(s)$ and $F(s)$

$$C_n(\Omega) = \frac{\varepsilon \prod_{k=1}^n (\Omega - zF_k/j)}{\varepsilon' \prod_{k=1}^{n_z} (\Omega - zP_k/j)} \quad (3.5)$$

Then we can generate the vector:

$$F'(\Omega_i) = C_n(\Omega_i) \cdot \prod_{k=1}^{n_z} (\Omega_i - zP_k/j) \quad (3.6)$$

We can find the coefficient of polynomial $F'(\Omega)$ by fitting $F'(\Omega_i)$ with a polynomial of order n . Then we could find the roots $\Omega_{F,k}$ of $F'(\Omega)$ with the following equation:

$$\Omega_{F,K} = \frac{zF_K}{j} \rightarrow zF_K = j\Omega_{F,K} \quad (3.7)$$

Finally, we can generate the characteristic polynomials from their roots (zP_k, zF_k). What's more, it is worth mentioning that if $n - n_z$ is even, $P(s)$ must be multiplied by j .

Until now, the evaluation of polynomials is done and we have already obtained the characteristic polynomials that defines the required response in the normalized low-pass domain.

3.2 General Configuration of Extraction with NRN

To get the scattering parameters, we should additionally define another polynomial through Feldtkeller equation, $E(s)$ is defined once $P(s)$ and $F(s)$ are known:

$$\frac{P(s)P(s)^*}{\varepsilon^2} + \frac{F(s)F(s)^*}{\varepsilon_r^2} = E(s)E(s)^* \quad (3.8)$$

Then we can derive the scattering parameters from the characteristic polynomials.

$$S_{11}(s) = \frac{F(s)/\varepsilon_R}{E(s)}, S_{21} = \frac{P(s)/\varepsilon}{E(s)}, S_{22}(s) = \frac{F_2(s)/\varepsilon_R}{E(s)} \quad (3.9)$$

When $n_z < n$: $\varepsilon_R = 1$

When $n_z = n$ (*fully canonical condition*)

$$\varepsilon_r = \frac{\varepsilon}{\sqrt{\varepsilon^2 - 1}} \quad (3.10)$$

With obtained scattering parameters of the characteristic polynomials, since we have chosen to realize an extracted-pole filter, we could now perform the synthesis of inline extracted-pole topology.

3.2 General Configuration of Extraction with NRN

Actually the synthesis of the low-pass prototype called “extracted-pole filters” is based on the subsequent extraction of the circuit elements from

3.2 General Configuration of Extraction with NRN

the $[ABCD]$ matrix evaluated by the characteristic polynomials obtained from the requirements, as shown in Fig.3.1.

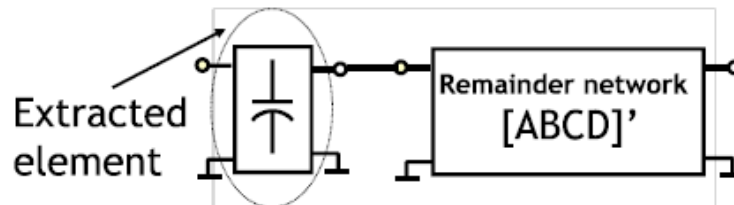


Figure 3.1: Subsequent extraction of the circuit elements from the $[ABCD]$ matrix

It is worth mentioning that extraction of transmission zeros (what we call “extracted poles”) must be suitably prepared by extracting before a frequency invariant component.

Then we have generally two basic approach for the synthesis of the low-pass prototype of the extracted-pole filter: extraction of zeros by phase shifters and extraction of zeros by non-resonating nodes (NRN).

Actually, a NRN is a node connected to ground through a frequency-invariant reactance. Obviously a NRN can be also represented as a frequency-invariant susceptance with value B_{nrn} (positive or negative). The introduction of NRNs in circuits brings several benefits, as shown in Fig.3.2.

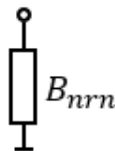


Figure 3.2: frequency-invariant susceptance with value B_{nrn}

3.2 Synthesis of the Low-Pass Prototype

Firstly, there is not a typical limit on the number of NRNs in a circuit since it will not affect the filter order, which means that NRNs allows to increase the number of transmission zeros for a given number of resonators (given order of a filter). Secondly, since NRNs are frequency-invariant, de-normalization will not change the value of NRNs. Consequently, the synthesis of filters with NRNs can be performed in the low pass domain.

However, we should pay attention that the coupling matrix is not meaningful with the introduction of NRNs.

The general configuration of extraction with NRN is shown in Fig.3.3:

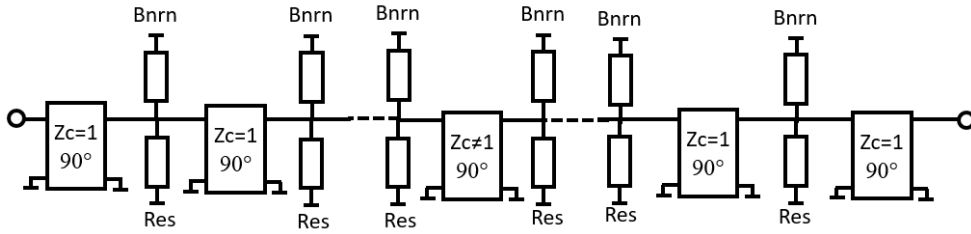


Figure 3.3: General configuration of extraction with NRN

B_{nrn} represents non-resonating elements, Res represents resonators, the coupling elements are phase shifters

The resonators in the figure can be either series resonators or shunt resonators. They are represented with equivalent slope parameter:

$$X_{eq} = \omega_{ris}L(\text{series}) \quad (3.10)$$

$$B_{eq} = \omega_{ris}C(\text{shunt}) \quad (3.11)$$

and resonating frequency f_{ris} .

3.3 Synthesis of the Low-Pass Prototype

The phase shifters are approximated by a transmission line with characteristic impedance Z_c and electrical length $\phi = \beta L$. When $\phi = 90^\circ$, the phase shifters become impedance inverters for series models with $K = Z_c$, which can be also considered as an admittance inverter for shunt models.

3.3 Synthesis of the Low-Pass Prototype

There are several methods to perform synthesis of the extracted-pole low-pass prototype, generally based on subsequent elements extractions. These methods are however affected by inaccuracies due to the accumulation of round off errors. To overcome these limitation, a very accurate synthesis method has been recently introduced in the literature [3]. Here we will give a brief introduction to this theory, which provides a simpler and more accurate synthesis method for inline extracted-pole low-pass prototype.

This method could be generally divided into two basic steps. The first step actually is the coupling-matrix synthesis (CM synthesis) method for canonical cross-coupled configuration, no matter which configuration is used. The literature [4] takes transversal network as an example. Based on the method introduced in the literature [4], we could get the synthesized result including $n + 2$ CM and capacitance matrix of the same dimension $C = \text{diag}(0,1,1, \dots, 1,1,0)$.

The second step is to transform the synthesized prototype obtained into the wheel form and then convert matrices M_{wheel} and C to the inline extracted-pole topology. Actually, no matter which kind of prototype is used, we can transform it into a wheel prototype based on the algorithm in the literature [4], which is briefly shown in the following:

Assuming that M_{full} is a generic $n + 2$ CM, $(0 (source), 1, \dots, n, n + 1 (load))$ are the indexes for its rows and columns and M_{wheel} is the needed wheel matrix.

3.3 Synthesis of the Low-Pass Prototype

$$M = M_{full}$$

for $k = 1:n - 1$

for $j = k + 1:n$

Annihilate element $M_{k-1,j}$ using element $M_{k,j}$ as pivot: (3.11)

$$\text{rotation angle } \vartheta_r = -\tan^{-1}\left(\frac{M_{k-1,j}}{M_{k-1,k}}\right)$$

Next j

Next k

$$M_{wheel} = M$$

Note that, matrix C is not changed by the transformation from M_{full} to M_{wheel} , which means it is equal to the synthesized result in the coupling-matrix synthesis. With matrices M_{wheel} and C , we could transform the wheel topology into the inline extracted-pole topology through the algorithm in the literature [3], which is based on the triplet extraction method. The algorithm of transformation from wheel prototype to inline extracted-pole topology is shown in Fig.3.4.

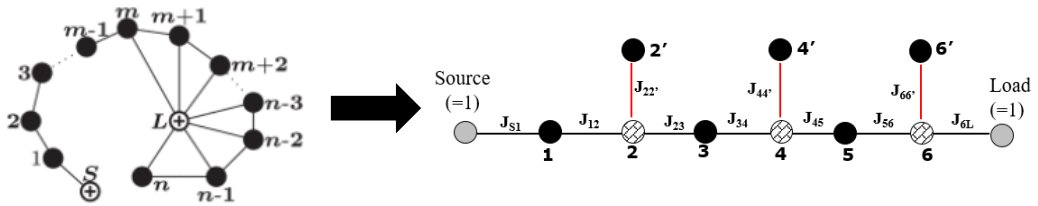


Figure 3.4: Transformation from wheel prototype to inline extracted-pole topology

3.3 Synthesis of the Low-Pass Prototype

This algorithm consists of $n - x$ matrix rotation and one Delta-to-star (D2S, described in the literature [9]) transformation for each finite transmission zeros (x represents x th resonant node). The matrix rotation is used to obtain a triplet $[x - 1, x, x + 1]$ contains a transmission zero f_x^i . Node t could be the resonant node $x - 1$, source node, or the NRN of an extracted-pole block created in the previous extraction. The obtained triplet is shown in Fig.3.5.

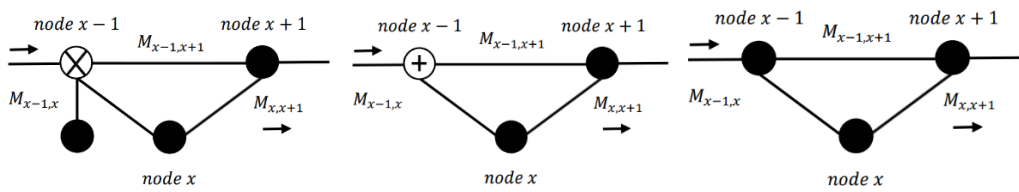


Figure 3.5: Obtained triplet from $n - x$ matrix rotation (resonant node $x - 1$, source node, NRN of an extracted-pole block created in the previous extraction)

Then we could perform D2S transformation to derive inline extracted-pole topology from obtained triplets above, which is shown in Fig.3.6:

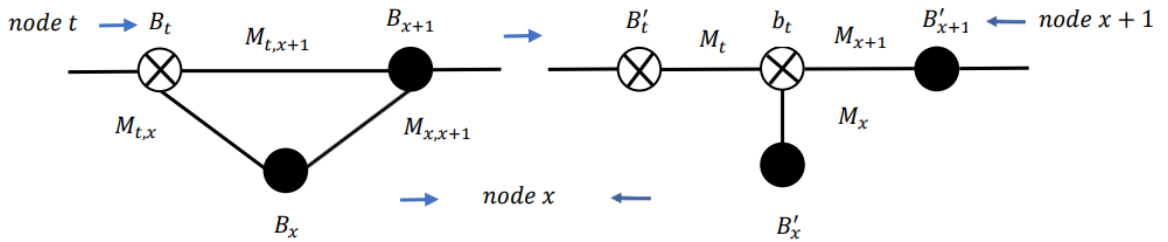


Figure 3.6: D2S transformation

3.3 Synthesis of the Low-Pass Prototype

$$B'_t = B_t - \frac{M_{t,x}M_{t,x+1}}{M_{x,x+1}} \quad (3.12)$$

$$B'_x = B_x - \frac{M_{t,x}M_{x,x+1}}{M_{t,x+1}} \quad (3.13)$$

$$B'_{x+1} = B_{x+1} - \frac{M_{t,x+1}M_{x,x+1}}{M_{t,x}} \quad (3.14)$$

$$M_t = M_{t,x} + M_{t,x+1} + \frac{M_{t,x}M_{t,x+1}}{M_{x,x+1}} \quad (3.15)$$

$$M_x = M_{t,x} + M_{x,x+1} + \frac{M_{t,x}M_{x,x+1}}{M_{t,x+1}} \quad (3.16)$$

$$M_{x+1} = M_{t,x+1} + M_{x,x+1} + \frac{M_{t,x+1}M_{x,x+1}}{M_{t,x}} \quad (3.17)$$

$$b_t = -M_t - M_x - M_{x+1} \quad (3.18)$$

Perform the D2S conversion for each triplet, then we can get the required inline extracted-pole topology, as shown in Fig.3.7.

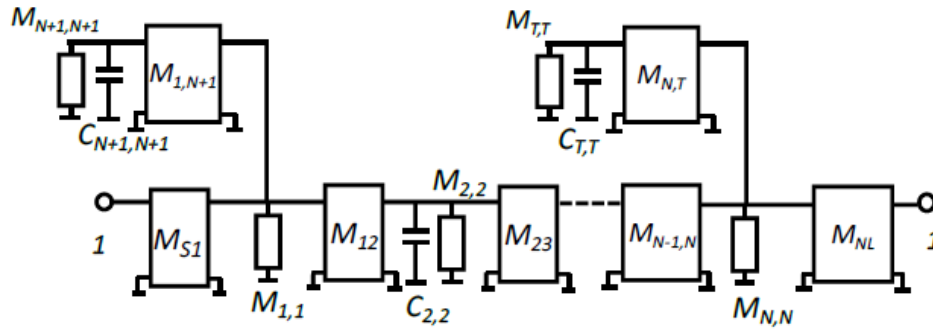


Figure 3.7: Synthesized equivalent circuit of the extracted pole filter

3.4 De-normalization of the Low-Pass Prototype

$M_{k,m}$ are ideal admittance inverter, $M_{k,k}$ are frequency-invariant susceptances, C_k are capacitors.

It is worth mentioning that the obtained synthesis equivalent circuits are intrinsically redundant, which means we could have infinite possible solutions. Thanks to the introduction of Generalized Coupled Coefficients (GCC) [5], we have the tools to deal with the redundancy. Actually the number of GCC is lower than the number of circuit variables, and GCC could determine the filter response.

3.4 De-normalization of the Low-Pass Prototype

Before the de-normalization of the prototype, we should set a characteristic value for each pole-zero-pairs (PZP)

It is important that GCC can exploit the available degrees of freedom during the process of prototype de-normalization. Here we mainly discuss about the following two cases

- (1) Inverter parameters as prior parts
- (2) Resonator parameters as prior parts

In the first case, we firstly assign the parameters of inverters. Since there are only N degrees of freedom while there are actually $N + 1$ inverters, we can only set the value of N inverters. We set the values of all the inverters to Y_0 , except the central one, as shown in Fig.3.8.

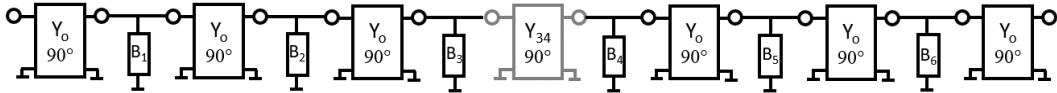


Figure 3.8: De-normalized filter with all the inverters equal to K_0 except the central one

3.4 De-normalization of the Low-Pass Prototype

Note that B_k can be either a resonant node or a non-resonant node, as shown in Fig.3.9.

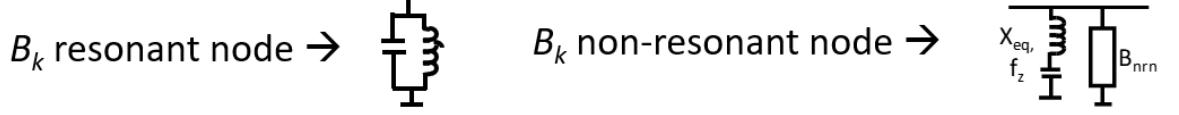


Figure 3.9: B_k as resonant nodes and B_k as non-resonant nodes

With the computed GCC from the synthesized filter, we can get the value of all the unknown parameters in the de-normalized filter.

For resonant nodes:

$$B_{eq} = B_k \quad (3.19)$$

For non-resonant nodes:

$$B_{nrn,k} = B_k \cdot \text{sign}(B_{nrn,k}) \quad (3.20)$$

$$X_{eq,k} = 1/(k_{z,k}^2 \cdot |B_{nrn,k}|) \quad (3.21)$$

Where $i = 1, 2, \dots, n$, $n = N/2$ for N even, $n = (N + 1)/2$ for N odd. The sign of susceptance B_i representing the i -th NRN is a result of the synthesized filter. Finally the value of the central inverter is also computed:

$$J_{n,n+1} = k'_{n,n+1} \sqrt{|B_n B_{n+1}|}, \begin{cases} n = N/2 & (N \text{ even}) \\ n = (N + 1)/2 & (N \text{ odd}) \end{cases} \quad (3.23)$$

3.4 De-normalization of the Low-Pass Prototype

According to the obtained results, we can notice that all the inverters except the central one ($J_{n,n+1}$) can be represented as 90° phase shifters with characteristic impedance equal to Y_c . Concerning the value of the central inverter $J_{n,n+1}$, it can be divided into two cases:

When $J_{n,n+1} > J_0$, we can transform the central inverter into a phase shifter with characteristic impedance K_0 and phase rotation $\theta \neq 90^\circ$, as shown in Fig.3.10.

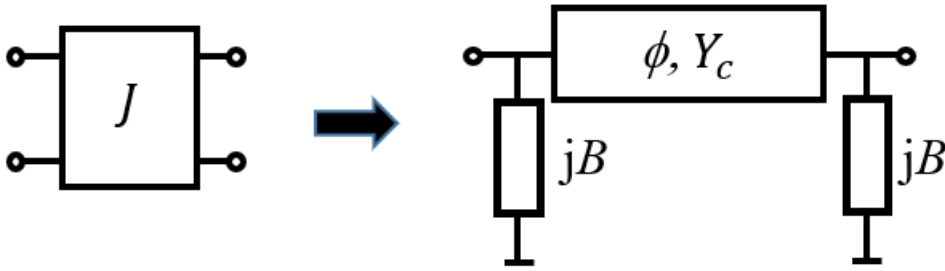


Figure 3.10: Transformation of the impedance inverter with $J > J_0$

B are frequency-invariant susceptances; θ is the electrical length of the transmission line and Y_c is the characteristic impedance of the transmission line. The relationship between them is:

$$\phi = \sin^{-1} \left(\frac{J_0}{J} \right) \quad (3.24)$$

$$B = \frac{J_0}{\tan(\phi)} \quad (3.25)$$

It is important that this transformation have interference on the adjacent nodes. If the adjacent node is a NRN, an additional B will be added in parallel to the adjacent B_{nrn} (note that the sign of B_{nrn} could be changed in some cases).

3.4 De-normalization of the Low-Pass Prototype

Concerning the effect of the transformation of the adjacent resonant node, we need to introduce the definition of Δ_z and k_z , which are characteristic parameters of a PZP block, as shown in Fig.3.11.

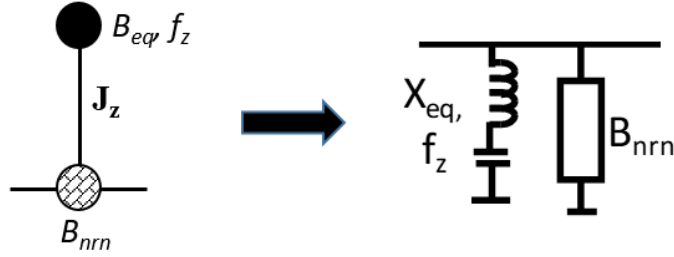


Figure 3.11: Configuration of the PZP block (shunt model)

$$k_z^2 = \frac{J_z^2}{B_{eq} \cdot |B_{nrn}|} = \frac{1}{X_{eq} \cdot |B_{nrn}|} \quad (3.26)$$

$$\Delta_r = \frac{f_r}{f_z} - \frac{f_z}{f_r} \quad (3.27)$$

$$\Delta_z = \frac{1}{X_{eq} B_{nrn}} = \text{sign}(B_{nrn}) \cdot k_z^2 \quad (3.28)$$

If the adjacent node is a resonant node, the effect is to change the resonating frequency of the resonant node. Meanwhile the ratio f_p/f_z is also changed, which is no longer related to k_z of PZP blocks.

When $J_{n,n+1} < J_0$, it is necessary to scale the node to get $J_{n,n+1} = J_0$. We define α as the scaling coefficient equal to the ratio between $J_{n,n+1}$ and J_0 :

$$\alpha = J_0/J_{n,n+1}, J'_{n,n+1} = \alpha J_{n,n+1} = J_0 \quad (3.29)$$

$$J'_{n-1,n} = \alpha J_{n-1,n} = \alpha \quad (3.30)$$

$$X'_{eq,n} = X_{eq,n}/\alpha^2, B'_{nrn,n} = \alpha^2 B_{nrn,n} \quad (3.31)$$

3.4 De-normalization of the Low-Pass Prototype

When we have got $J'_{n-1,n} > J_0$, we can apply the transformation reported above to obtain a phase shifter from an impedance inverter.

In the second case, we assign the prior to the resonator parameters, which are B_{eq} and X_{eq} , as shown in Fig.3.12.

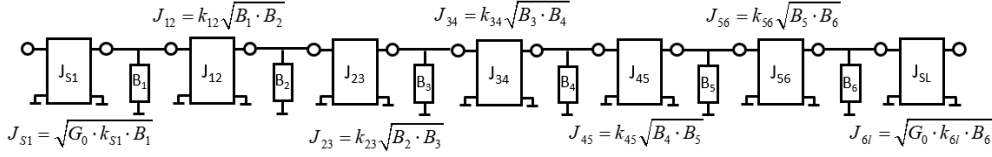


Figure 3.12: De-normalized filter with all the resonators assigned (B_{eq} and X_{eq})

The degree of freedom introduced by GCC is N and the number of resonators is also N . We can therefore assign the parameters B_{eq} and X_{eq} of all the resonators.

If the node i is resonant,

$$B_i = B_{eq} \quad (3.32)$$

If the node i is non-resonant,

$$B_i = |B_{nrn,i}| = \frac{1}{(k_{ii}^2 \cdot X_{eq})} \quad (3.33)$$

After determining the parameters of resonators, the inverters can be evaluated from

$$J_{i,i+1} = k_{i,i+1} \sqrt{B_i \cdot B_{i+1}} \quad (3.34)$$

3.4 De-normalization of the Low-Pass Prototype

Actually this solution is convenient and commonly used for waveguide cavity resonators since couplings are realized with irises and rejection resonators with stub.

Until now, we have got the de-normalized filter suitable for physical implementation, which will be discussed in the next chapter.

Chapter 4

Realization of An Extracted-Pole Filter in Coaxial Technology

In this chapter, we will discuss all the steps taken in order to realize an extracted-pole band-stop filter in a coaxial cavity structure, from the initial requirements to the geometrical dimension of final physical filter.

4.1 Assignment of the Electrical Specification

The electrical specifications for the filter are listed as following:

- Stopband: $905 - 912 \text{ MHz}$, $A_{min} = 45 \text{ dB}$
- Passband: $872.5 - 902 \text{ MHz}$, $RL = 23 \text{ dB}$

As shown in the specification, the required filter has one passband and one single band, which could be called “single sided” filter. For this kind of filters, we could both consider it as a bandstop filter or a bandpass filter.

For a bandpass filter, with the filter order determined (np), we could assign the number and location of transmission zeros, and the number of transmission zeros could not be larger than filter order ($\leq np$), and we

4.1 Assignment of the Electrical Specification

could determine the location of reflection zeros whose number is equal to filter order np and produce equal ripple S_{11} in the passband.

For a bandstop filter, with the filter order determined (np), we could assign the number and location of reflection zeros, and the number of reflection zeros could not be larger than filter order ($\leq np$), and we could determine the location of transmission zeros whose number is equal to filter order np and produce equal ripple S_{21} in the stopband.

Here we determine to choose the bandstop filter. Actually, both the two methods could be used to realize a fully canonical filter with the number of transmission zeros equal to the filter number. In the first case (bandpass filter), assuming the filter order is 4, we will have 4 transmission zeros and 4 reflection zeros. However, in the second case (bandstop filter), we will have 4 transmission zeros, and the number of reflection zeros could be adjusted (≤ 4). This means that the first case does not allow any degrees of freedom once the filter order is assigned. However, the second case allows the free choice of the number of reflection zeros, which could benefit procedures.

Additionally, we should also consider whether the synthesized filter is realistic or not. Assuming the filter order is 4, in the first case, we have a bandpass filter with 4 transmission zeros and 4 reflection zeros. To satisfy the electrical specifications ($A_{min} = 45dB$ in the stopband), we could obtain the synthesized filter, as shown in Fig.4.1:

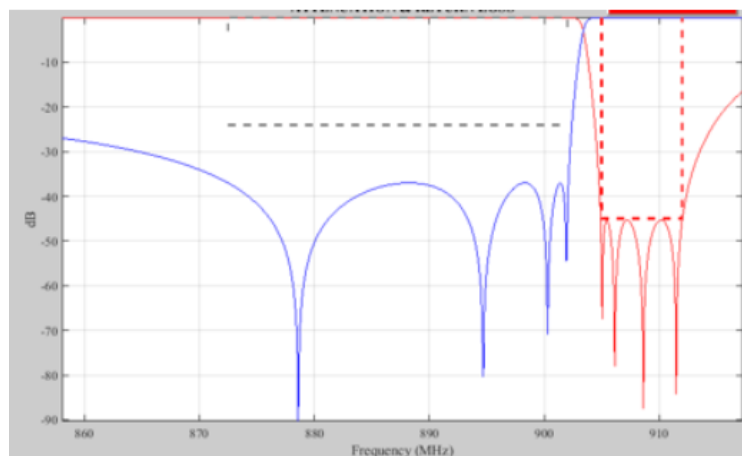


Figure 4.1: Synthesized bandpass filter

4.1 Assignment of the Electrical Specification

Note that, although both the return loss in the passband and attenuation in the stopband is satisfied, the return loss is much larger than requested, which the synthesized filter is not very realistic. An example is shown in Fig.4.2:

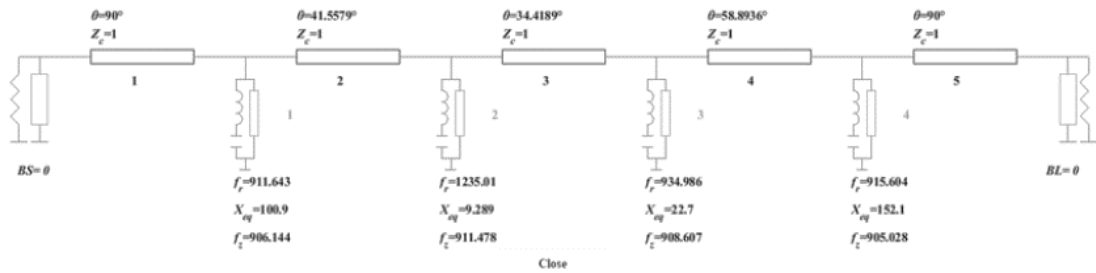


Figure 4.2: Equivalent circuit of a synthesized bandpass filter

From the equivalent circuit, we need to realize X_{eq} whose value is very large, the maximum X_{eq}/Z_0 is 152.1, which is almost unrealistic.

On the other case, when we choose to use a bandstop filter to realize 4 transmission zeros, we could freely choose the number of reflection zeros. It means that we could assign less reflection zeros in order to have a not very large return loss (still satisfy the requirements). For example, Fig.4.3 shows the response with 2 reflection zeros.

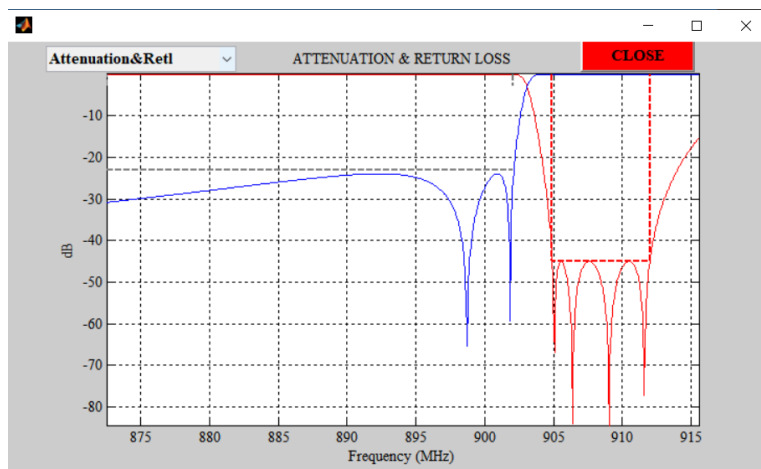


Figure 4.3: Synthesized bandpass filter with 2 reflection zeros

4.1 Assignment of the Electrical Specification

As shown in the figure above, the return loss is not so large, and it still satisfies the specifications. Such a synthesized filter is more realistic than the first case. Actually, the maximum X_{eq}/Z_0 could be much lower, which will be shown in the following chapters.

In conclusion, we choose to use a bandstop filter with two reflection zeros:

- Bandstop filter, Filter order 4, reflection zeros 2

Concerning the synthesis of bandstop filter, the literature [8] introduced a direct synthesis of bandstop filters. A bandstop filter can be designed as a folded canonical structure that is used to design elliptic bandpass filter.

We choose a generalized Chebyshev filter with order equal to 4, and assign two reflection zeros,

To start the design, we assign several variables. The stopband is centred at w_0 and the lower and upper limit of the band are w_1 and w_2 . The rejection level in the stopband is called A and the return loss in the passband is called RL . We could use these parameters to determine the filter order and number and location of reflection zeros in the bandstop filter (not transmission zeros in the bandpass case). This step of the bandstop filter is identical to that of the bandpass filter. To satisfy the requirements in this thesis and have equal ripple (use a generalized Chebyshev filter), we have the following result.

Then the generalized Chebyshev filtering function $F_N(\omega)$ is given by

$$F_N(\omega) = \cosh \left[\sum_{k=1}^{k=N} \cosh^{-1} \left(\frac{\omega - \frac{1}{\omega_k}}{1 - \frac{\omega}{\omega_k}} \right) \right] = \frac{P_N(\omega)}{D_N(\omega)} \quad (4.1)$$

Note that, it is very important that ω_k are the positions of the reflection zeros in the bandstop filter. The denominator $D_N(\omega)$ is a polynomial of degree equal to the number of reflection zeros, equal to 2 in this case. The numerator $P_N(\omega)$ is a polynomial of degree equal to the number of filter order. The obtained denominator and numerator is shown in the following:

4.1 Assignment of the Electrical Specification

$$D_N(\omega) = \prod_{k=1}^{N_z} \left(1 - \frac{\omega}{\omega_k}\right) = \sum_{i=0}^{N_z} d_i^{(N_z)} \omega^i \quad (4.2)$$

$$P_{m+1}(\omega) = \sum_{i=0}^{m+1} a_i^{(m+1)} \omega^i \quad (4.3)$$

$$a_i^{(m+1)} = -S(m, m+1)a_i^{(m-1)} - a_i^{(m)} \times \left(\frac{1}{\omega_{m+1}} + \frac{S(m, m+1)}{\omega_m}\right) + 2a_{i-1}^{(m-1)} \frac{S(m, m+1)}{\omega_m} + a_{i-1}^{(m)} \times (1 + S(m, m+1)) - a_{i-2}^{(m-1)} \frac{S(m, m+1)}{\omega_m^2} \quad (4.4)$$

$$S(m, m+1) = \sqrt{\frac{1 - \frac{1}{\omega_{m-1}^2}}{1 - \frac{1}{\omega_m^2}}} \quad (4.5)$$

The coefficient of the two polynomials P_0 and P_1 are $a_0^{(0)} = 1$, $a_0^{(1)} = -1/\omega_1$, and $a_1^{(1)} = 1$.

It is worth mentioning that for a bandpass case with RL, assigned transmission zeros and a bandstop case with in-band rejection (equal to RL), reflection zeros (same location as transmission zeros in the bandpass case), the final filtering function remains the same.

To be more exact, when we want to perform the evaluation of polynomials in a bandstop filter, we firstly perform the evaluation of polynomials of a bandpass filter with pass and stop bands exchanged. Then we just need to exchange the F and P polynomials obtained in the bandpass filter, so that the assigned return loss in the bandpass will become the imposed attenuation in the stop band. Consequently the roles of S_{11} and S_{21} are switched when going from bandpass to bandstop.

After the evaluation of polynomials, we could compute the scattering parameters, which is shown in Fig.4.4:

4.2 Synthesis and De-normalization of a Low-Pass Prototype

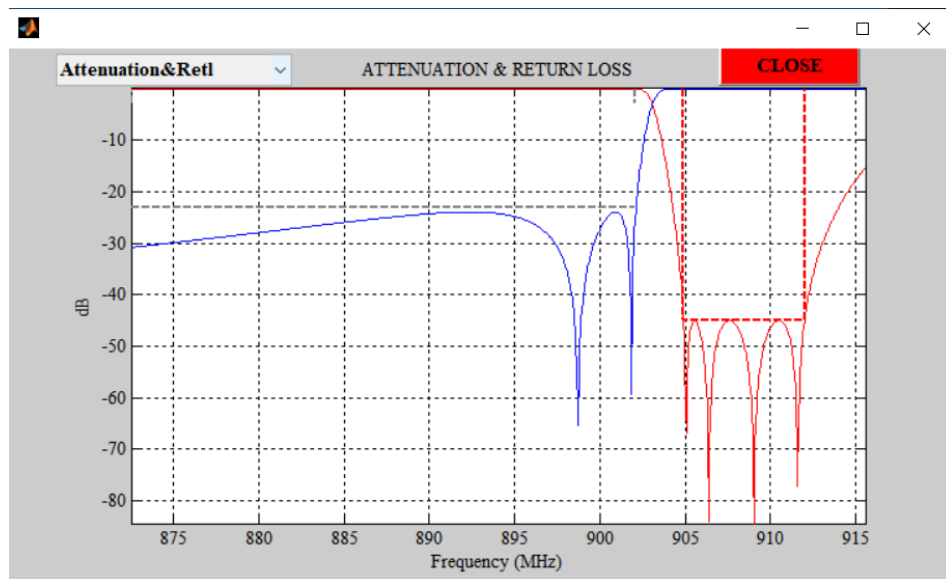


Figure 4.4: Obtained final results of scattering parameters

4.2 Synthesis and De-normalization of a Low-Pass Prototype

Thanks to the software Filines, all the steps of synthesis of a low-pass prototype could be done through it, which saves a lot of time. With the scattering parameters and transmission zeros known, we need to choose the suitable extracted-pole sequence during the synthesis process, since it has huge effects on parameters of the final de-normalized circuit. Here we choose the extracted-pole sequence with minimum X_{eq} in the de-normalized circuit. The routing scheme of the synthesized filter is shown in Fig.4.5:

4.2 Synthesis and De-normalization of a Low-Pass Prototype

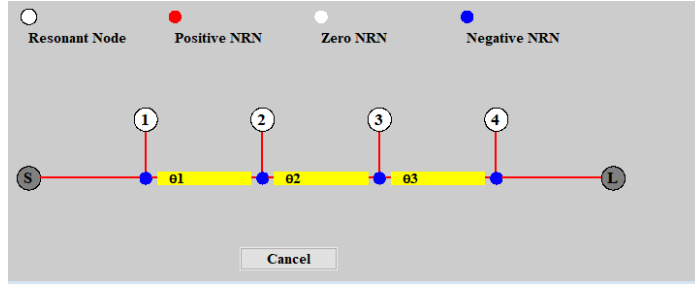


Figure 4.5: Routing scheme of the synthesized filter

From the two type of equivalent circuit (shunt/series), in this thesis we choose shunt equivalent circuit, which has benefits on the latter physical implementation. Regarding the degrees of freedom introduced by GCC, we choose to assign all the admittance inverter equal to the external load except the middle one, the result is shown in Fig.4.6:

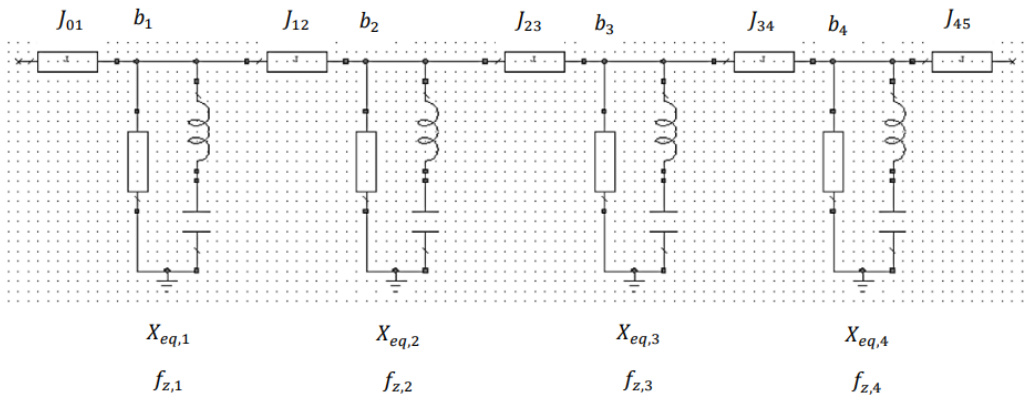


Figure 4.6: Equivalent circuit of the filter with assigned inverters

$$J_{01} = J_{12} = J_{34} = J_{45} = 1, J_{23} = 1.0011 \quad (4.6)$$

$$b_1, b_2, b_3, b_4 = [-0.56536, -1.217, -1.1421, -0.75837] \quad (4.7)$$

$$X_{eq,1}, X_{eq,2}, X_{eq,3}, X_{eq,4} = [48.0589, 48.5222, 71.7031, 56.0967] \quad (4.8)$$

$$f_{z,1}, f_{z,2}, f_{z,3}, f_{z,4} = [911.5916, 906.3929, 905.0577, 909.0465] \quad (4.9)$$

4.2 Synthesis and De-normalization of a Low-Pass Prototype

We can notice that for each invert, $J \geq 1$, it is already sufficient to replace admittance inverters with phase shifter, so there is no need to scale the nodes. Then we can perform the transformation from the admittance inverter J_{23} to the phase shifter ϕ_{23} with two shunt susceptance, imposing all the characteristic impedances equal to 1, as shown in Fig.4.7:

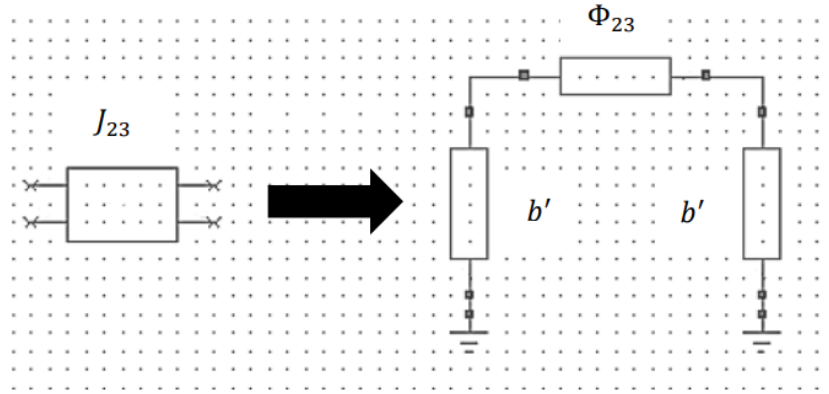


Figure 4.7: Transformation of the admittance inverter to the phase shifter

$$\phi_{23} = \sin^{-1} \left(\frac{1}{J_{23}} \right) = 87.37^\circ \quad (4.10)$$

$$b' = \frac{1}{\tan(\phi_{23})} = 0.0459 \quad (4.11)$$

Obviously, the adjacent susceptance will be changed:

$$b_2 = -1.217 + b' = -1.171, b_3 = -1.1421 + b' = -1.0962 \quad (4.12)$$

Then we can get the final scheme of the synthesized filter and compute frequency response (scattering parameters) with a circuit simulator, as shown in Fig.4.8 and Fig.4.9:

4.3 Physical Implementation with Coaxial Technology

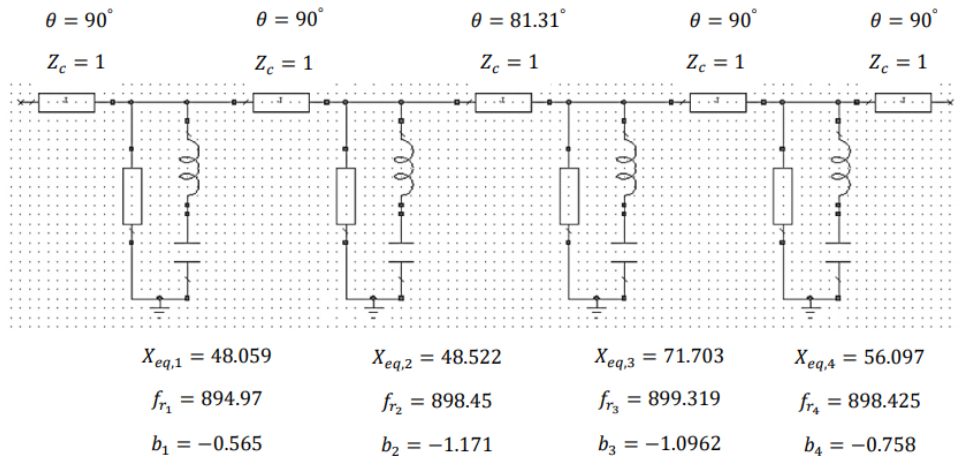


Figure 4.8: Final scheme of the synthesized filter

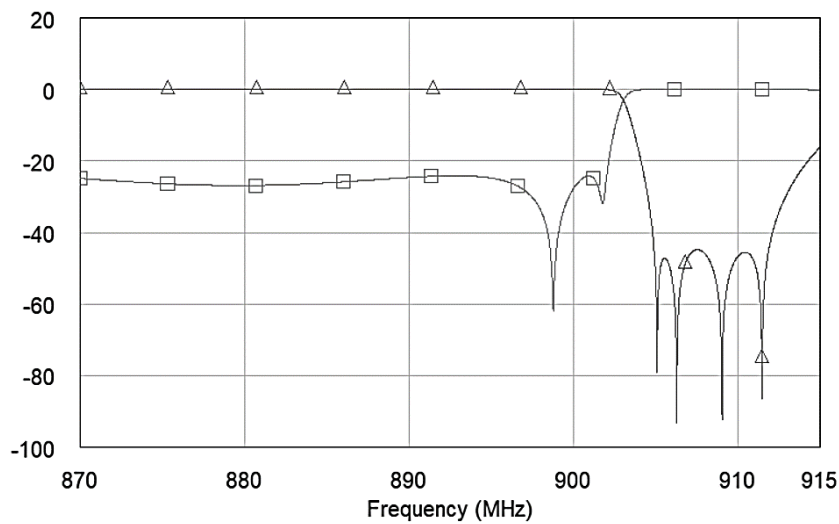


Figure 4.9: Computed frequency response (scattering parameters)

4.3 Physical Implementation with Coaxial Technology

The physical implementation is based on a concept called “Divide and Conquer”. Actually we can break the design of the whole filter into several pole-zero pairs (PZP) blocks. We dimension each PZP block, and the goal

4.3 Physical Implementation with Coaxial Technology

is to get the required parameters (f_z, X_{eq}, B_{nrn}) from each block as same as that imposed by the filter synthesis. This work is proceeded through HFSS.

HFSS (high frequency structure simulator) is a finite element method solver for electromagnetic structures. It uses the 3D finite element method to analyse the electromagnetic field distribution inside the microwave devices, and then obtains various required network parameters, i.e. scattering parameters.

The physical structure of a PZP block is shown in Fig.4.10:

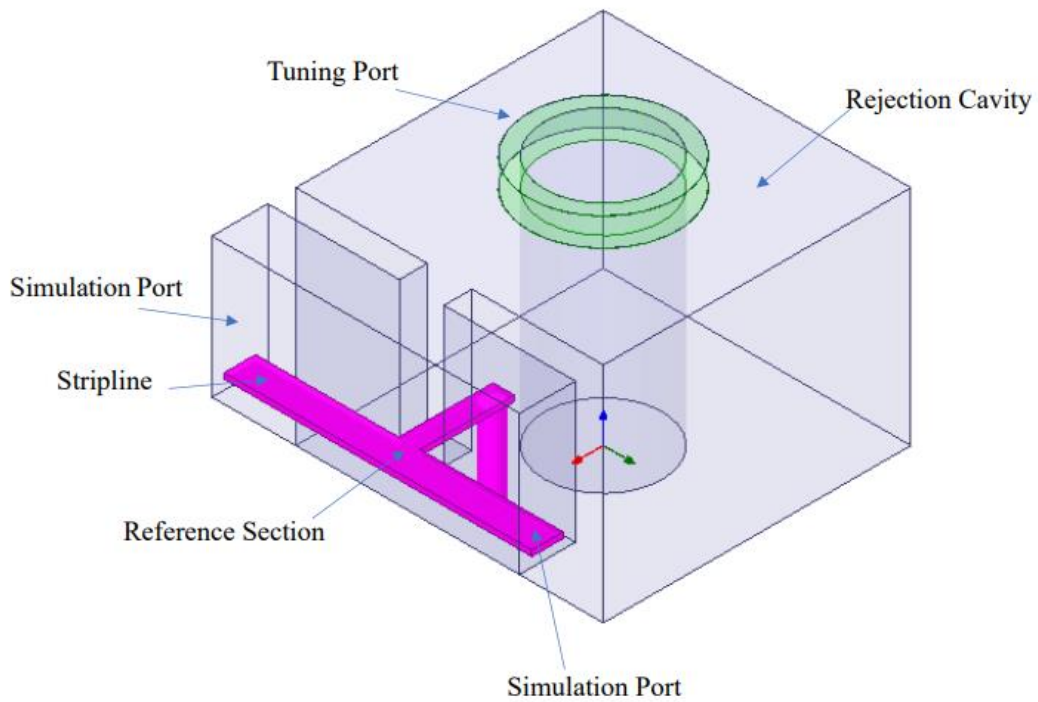


Figure 4.10: Physical model of the PZP block

The equivalent circuit of this kind of physical PZP block is shown in the Fig.4.11:

4.3 Physical Implementation with Coaxial Technology

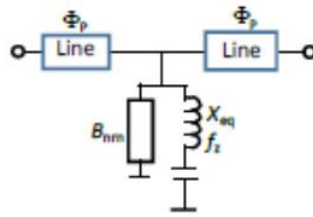


Figure 4.11: Shunt equivalent circuits

In the equivalent circuits, ϕ_p is the electrical length of the line, B_{nrn} is a frequency-invariant element, X_{eq} and f_z are the equivalent slope parameter and the resonance frequency of the rejection resonator.

Consequently, the equivalent circuits of the physical PZP block shown above is suitable for the realization of obtained synthesized filter. Then we could start the geometrical dimension of each block.

The basic component of the physical circuit is a coaxial rejection cavity. The cavity is coupled to the boxed stripline to satisfy the required inductance. To get required the negative susceptance of NRN, we have two solutions. Firstly, the loop shown in the figure has already creates a negative susceptance. Secondly, if the negative susceptance created by the loop is not enough, an additional short-circuited port could be added on the stripline, which will be discussed in later chapters.

To get suitable geometrical dimension of each block, we can divide the whole work into two general steps. The first step is to size the cavity to resonate in the required band (900MHz). The second step is to size the blocks one by one, to get required X_{eq} , B_{nrn} , f_z for each block. The variables used in the geometrical dimension process are reported in Fig.4.12 and Fig.4.13:

4.3 Physical Implementation with Coaxial Technology

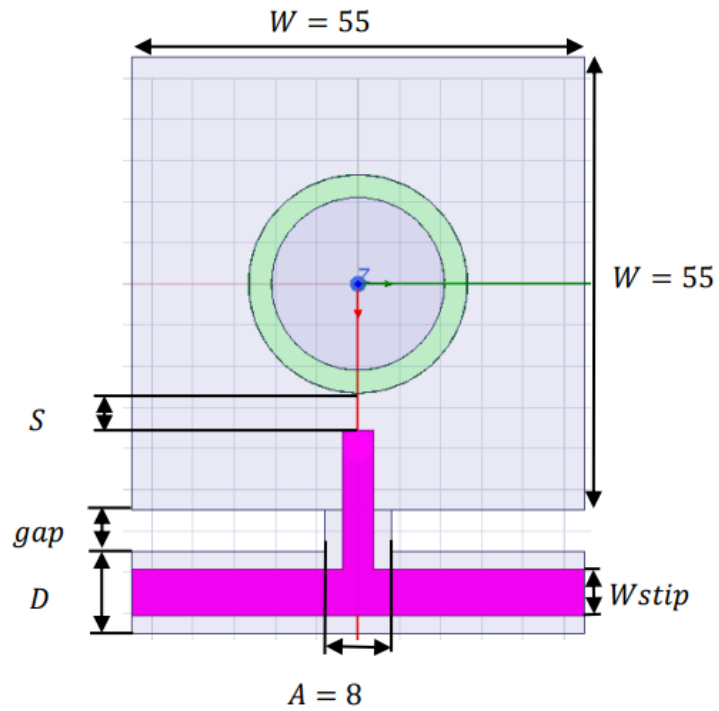


Figure 4.12: Dimension parameters of the model of PZP block

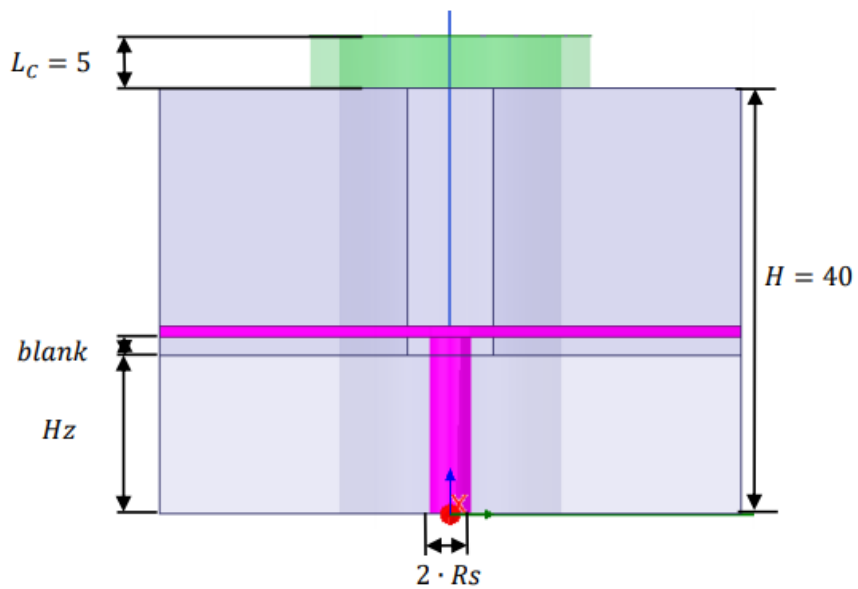


Figure 4.13: Dimension parameters of the model of PZP block

4.3 Physical Implementation with Coaxial Technology

The main challenge is that the number of variables during the dimension process is too large. It is really hard to determine how to change them due to the couplings among the variables. So we divide these variables into two kinds: global variables and local variables.

Global variable: variables that used to size the cavity to resonate in the required band (900MHz) and cannot be changed during the later process.

Local variable: variables that used to get required X_{eq}, B_{nrn}, f_z for each block.

4.3.1 Global variables

We choose $H, D, gap, Wstrip, blank$ as so-called global variables. The main reason is that the final filter uses an inline cascaded-block configuration, these variables of each block must be same for connection. If the variables are different, i.e., blank, the stripline will be misconnected, which will have bad effects on the final performance of filter. Then the remaining variables s, Rs are so-called local variables. All the variables are shown in Tab.4.1:

Global variables	$H, D, gap, Wstrip, blank$
Local variables	Rs, s

Table 4.1: Geometrical dimension variables in the design of PZP block

In addition, it is very important that we have not discussed about the characteristic impedance of the stripline, and it must be set to 50 Ohm. Actually, we find that all the local variables almost do not change the value of characteristic impedance of the stripline. It is because the change of local variables cannot affect the parameters of the stripline. To be exact, we analyse the relationship between local variables and characteristic impedance of the stripline with HFSS, the result is shown in Fig.4.14:

4.3 Physical Implementation with Coaxial Technology

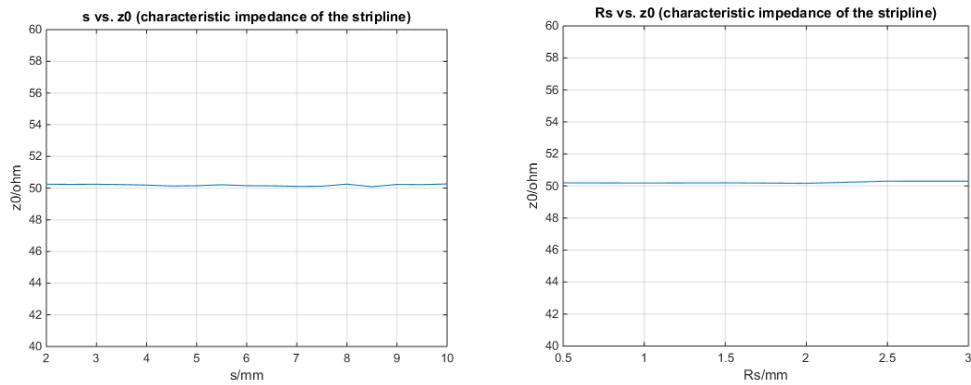


Figure 4.14: Relationship between s , R_s and Z_0 (characteristic impedance of the stripline)

Since the local variables almost do not affect the characteristic impedance, we can simply set the required value of characteristic impedance during the process of global variables. In conclusion, the local variables are determined to obtain a resonating frequency approximately equal to 900MHz and characteristic impedance equal to 50 Ohm .

We use HFSS to analyse the relationship between these variables and f_z (transmission zero) and the relationship between these variables and Z_0 (characteristic impedance of the stripline), the results are shown in Fig.4.15 to Fig.4.19:

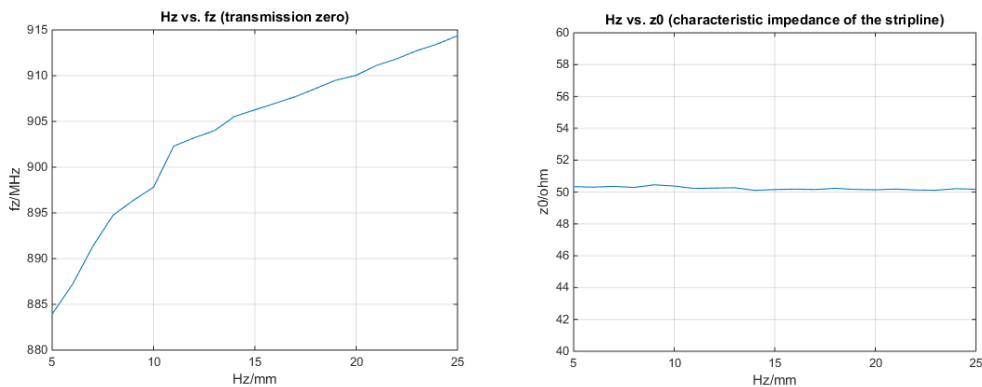


Figure 4.15: Relationship between H_z and f_z (transmission zero), Z_0 (characteristic impedance of the stripline)

4.3 Physical Implementation with Coaxial Technology

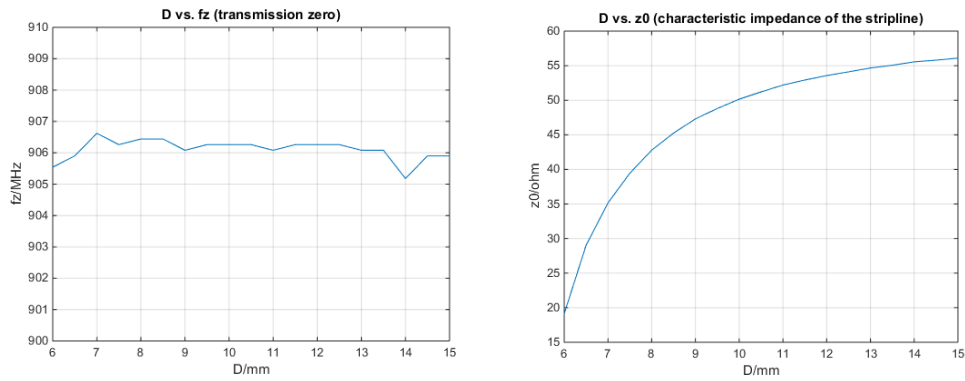


Figure 4.16: Relationship between D and f_z (transmission zero), Z_0 (characteristic impedance of the stripline)

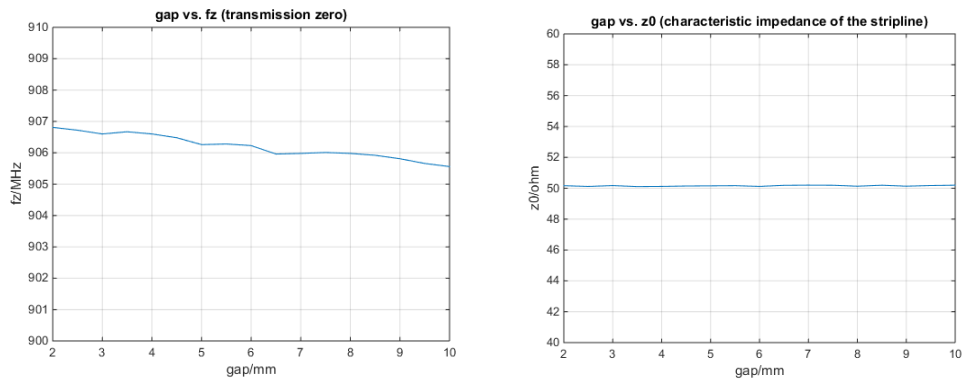


Figure 4.17: Relationship between gap and f_z (transmission zero), Z_0 (characteristic impedance of the stripline)

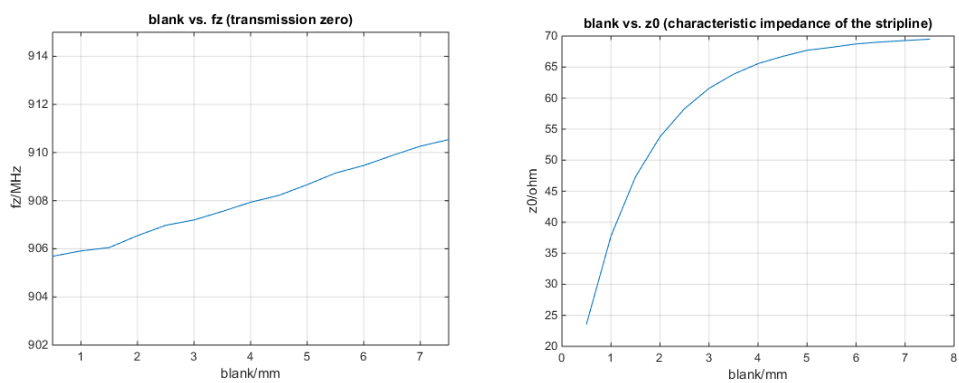


Figure 4.18: Relationship between $blank$ and f_z (transmission zero), Z_0 (characteristic impedance of the stripline)

4.3 Physical Implementation with Coaxial Technology

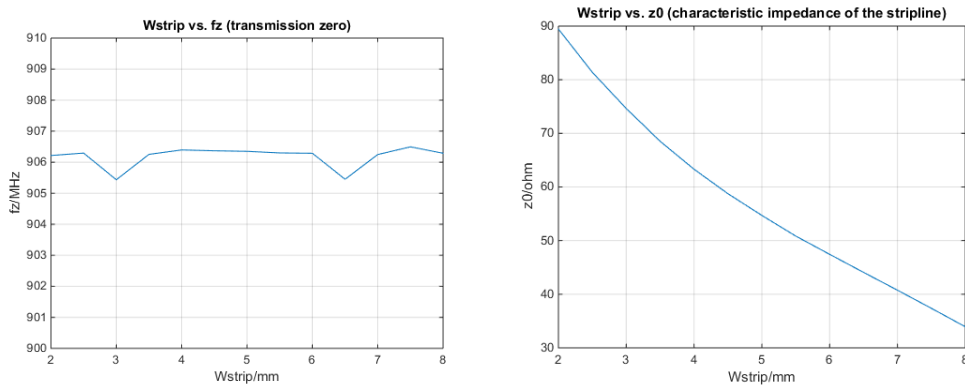


Figure 4.19: Relationship between $Wstrip$ and f_z (transmission zero), Z_0 (characteristic impedance of the stripline)

As shown in the figures, we can find that

- (1) f_z increase with the increase of hz , but Z_0 remains almost the same
- (2) D is opposite to f_z . When f_z increases, f_z remains almost the same while Z_0 increases.
- (3) With the increase of gap , Z_0 is unchanged and f_z is slowly decreasing.
- (4) With the increase of $blank$, both f_z and Z_0 is increasing.
- (5) When $Wstrip$ is increasing, f_z does not change a lot while Z_0 is decreasing quickly.

To satisfy the requirements of both f_z and Z_0 , firstly we change the value of Hz , gap to get required f_z . The reason is that Hz show large effects on f_z and almost no effect on Z_0 . Concerning the variable gap , although the change of f_z is not very large, but it is more significant than the change of Z_0 . Then we change the value of D , $blank$, $Wstrip$ to obtain the required value of characteristic impedance (50 Ohm).

It is worth mention that we use D for the determination of Z_0 rather than f_z . Actually it comes from the consideration the level of requirements. With the dimension of global parameters, we need to obtain an “exact” value of Z_0 and an “approximate” value of f_z . It is obvious because during the latter dimension of local parameters, Z_0 remains almost unchanged while f_z will definitely changes. So actually we just need a “range” of f_z and the exact value of f_z will be determined by local parameters.

4.3 Physical Implementation with Coaxial Technology

The value of global parameters is reported in Tab.4.2:

H_z	D	gap	$blank$	$Wstrip$
15	10	5	1.7	5.6

Stable 4.2: Assignment of global parameters

4.3.2 Local variables

Local variables are used to obtain exact values of X_{eq} and B_{nrn} for each block. In other words, we need to get a pair of (R_s, s) for each pair of (X_{eq}, B_{nrn}) .

Actually X_{eq}, B_{nrn} can be computed from the following relationships:

$$U = \frac{1}{2} Im \left\{ \frac{S_{21}}{S_{11}} \right\} \quad (4.13)$$

$$\Phi_p = -\frac{\angle(S_{12} - S_{11})}{2} \quad (4.14)$$

$$X_{eq} = -\frac{1}{2} f_z \left. \frac{\partial U}{\partial f} \right|_{f=f_z} \quad (4.15)$$

$$B_{nrn} = \left[X_{eq} \left(\frac{f_r}{f_z} - \frac{f_z}{f_r} \right) \right]^{-1} \quad (4.16)$$

Here we use shunt model since X_{eq} is positive and consequently we should compute ϕ_s, X_{eq} and B_{nrn} .

Then we can use post-process tuning to move the transmission zero f_z to the exact place of each block. Once the f_z is moved to the right place, the final step is to connect the blocks with suitable length, which can be computed from the synthesis result but maybe need to be modified due to frequency dispersion of the real transmission lines.

4.3 Physical Implementation with Coaxial Technology

The relationship between (R_s, s) and X_{eq} are shown in Fig.4.20 and Fig.4.21:

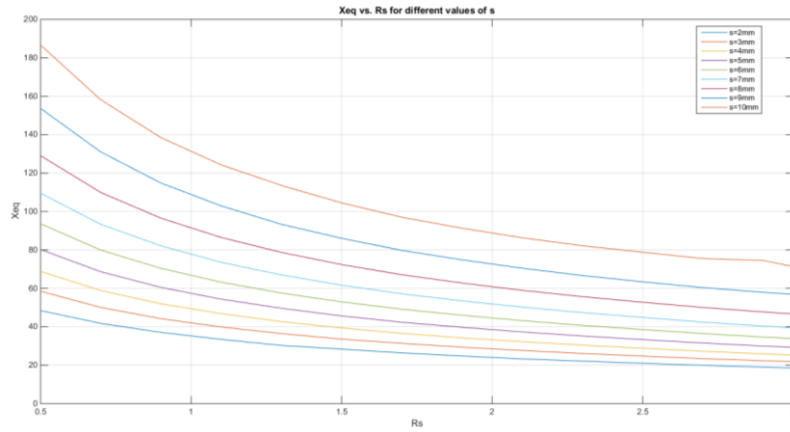


Figure 4.20: X_{eq} vs. R_s for different values of s

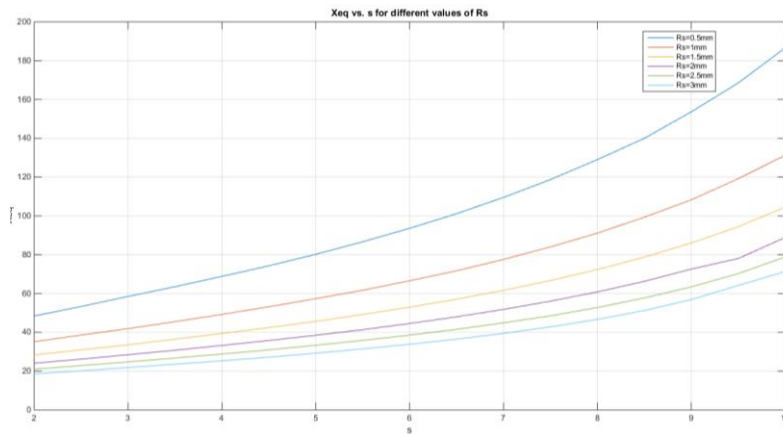


Figure 4.21: X_{eq} vs. s for different values of R_s

The relationship between (R_s, s) and B_{nrn} are shown in Fig.4.22 and Fig.4.23:

4.3 Physical Implementation with Coaxial Technology

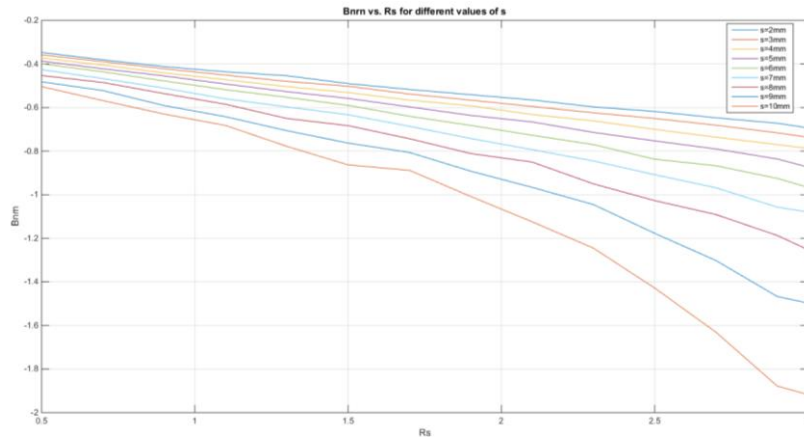


Figure 4.22: B_{nrn} vs. R_s for different values of s

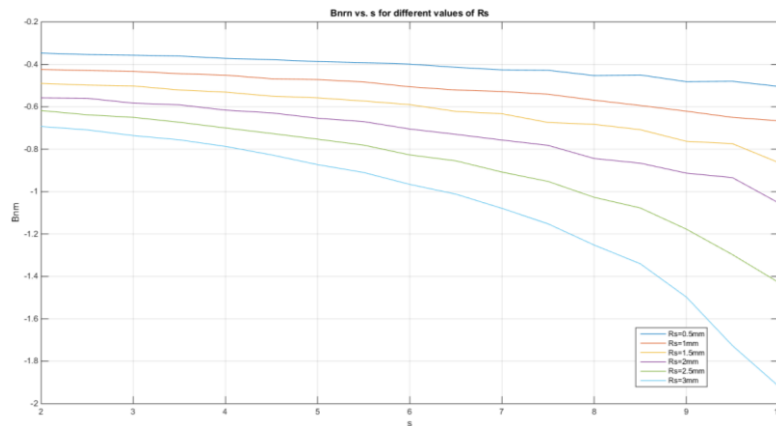


Figure 4.23: B_{nrn} vs. s for different values of R_s

According to the analysis above, we know that the solution plane is a plane of R_s vs. s . Firstly we can find the required X_{eq} for each block in the figures above. We get the solution pairs (R_s, s) for X_{eq} , and draw a curve in the plane R_s vs. s with constant X_{eq} . Similarly, we get the solution pairs (R_s, s) for B_{nrn} , and draw a curve in the plane R_s vs. s with constant B_{nrn} . The intersection of the two curves is the solution pair (R_s, s) for each (X_{eq}, B_{nrn}) .

4.3 Physical Implementation with Coaxial Technology

We repeat the procedures discussed above for each block, the requirements are shown in Tab.4.3 and the intersections of the four blocks are shown in Fig.4.24 to Fig.4.27:

	X_{eq}	B_{nrn}
Block1	48.059	-0.565
Block2	48.522	-1.171
Block3	71.703	-1.0962
Block4	56.097	-0.758

Stable 4.3: Required (X_{eq}, B_{nrn}) for each block

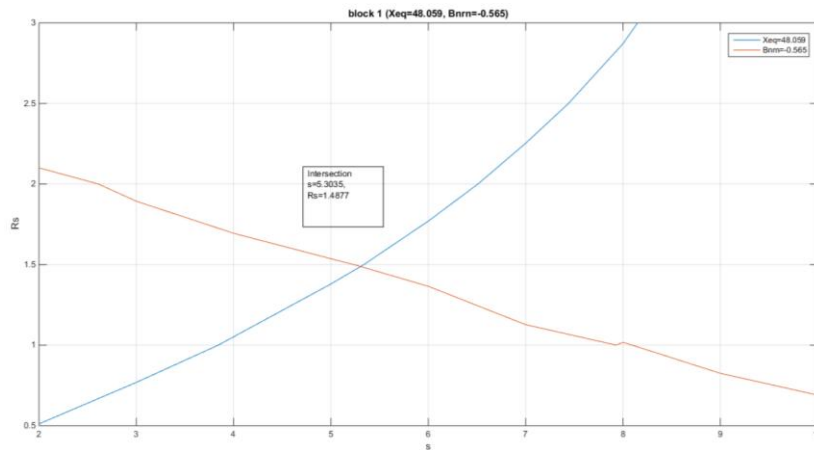


Figure 4.24: s vs. R_s for block 1

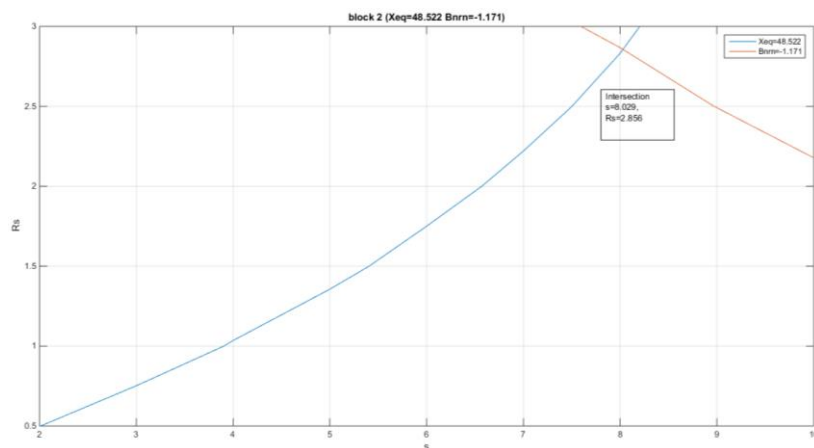


Figure 4.25: s vs. R_s for block 2

4.3 Physical Implementation with Coaxial Technology

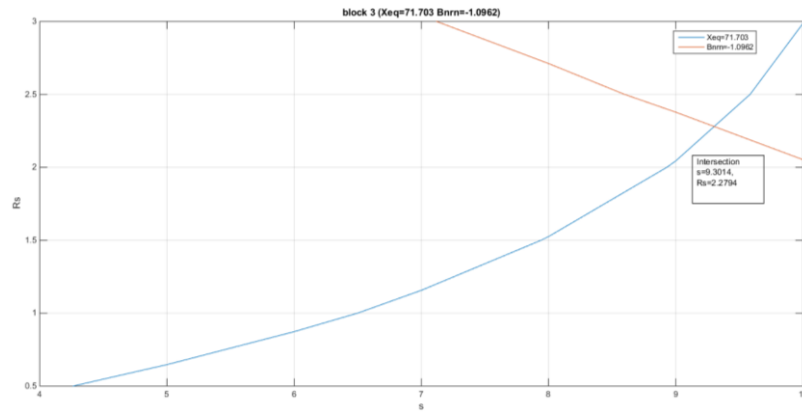


Figure 4.26: s vs. R_s for block 3

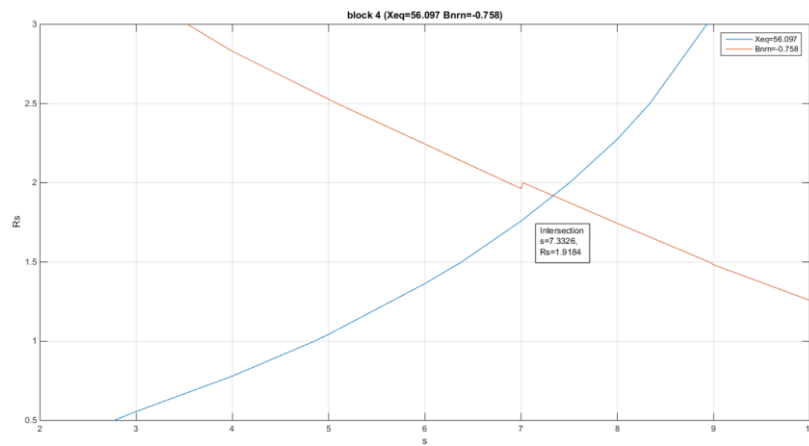


Figure 4.27: s vs. R_s for block 4

The intersections in the four figures are the (R_s, s) solutions for the blocks are shown in Tab.4.4:

	Block1	Block2	Block3	Block4
s	5.3035	8.029	9.3014	7.3326
R_s	1.4877	2.856	2.2794	1.9184

Stable 4.4: (R_s, s) solution pairs for each block

With all the obtained parameters, we use HFSS to perform post-processing tuning and move the transmission zeros to the right places, and then compare the scattering parameters of each block with that of synthesized filter. The results are shown in Fig.4.28 to Fig.4.31.

4.3 Physical Implementation with Coaxial Technology

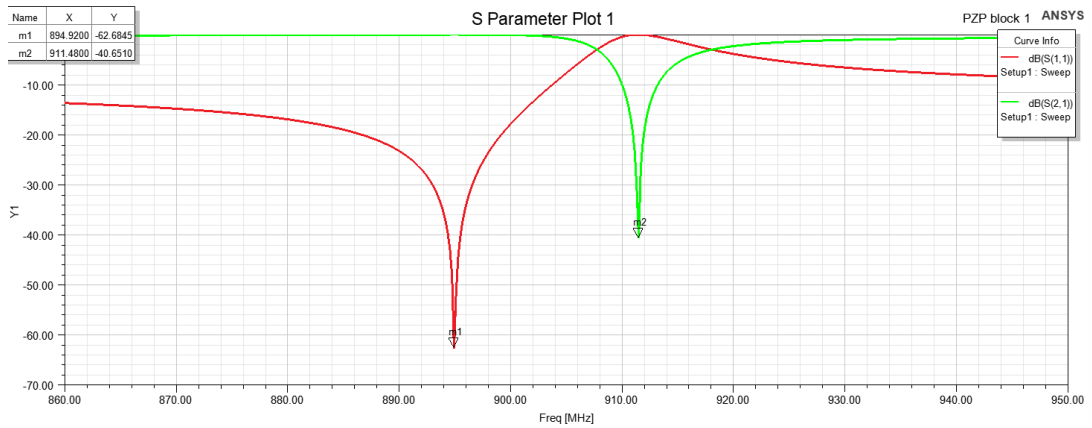


Figure 4.28: Scattering parameters of block 1

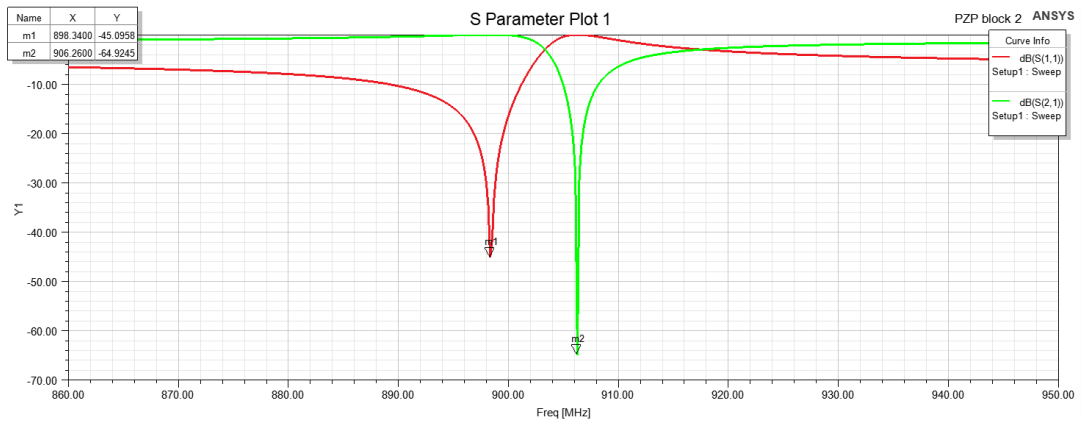


Figure 4.29: Scattering parameters of block 2

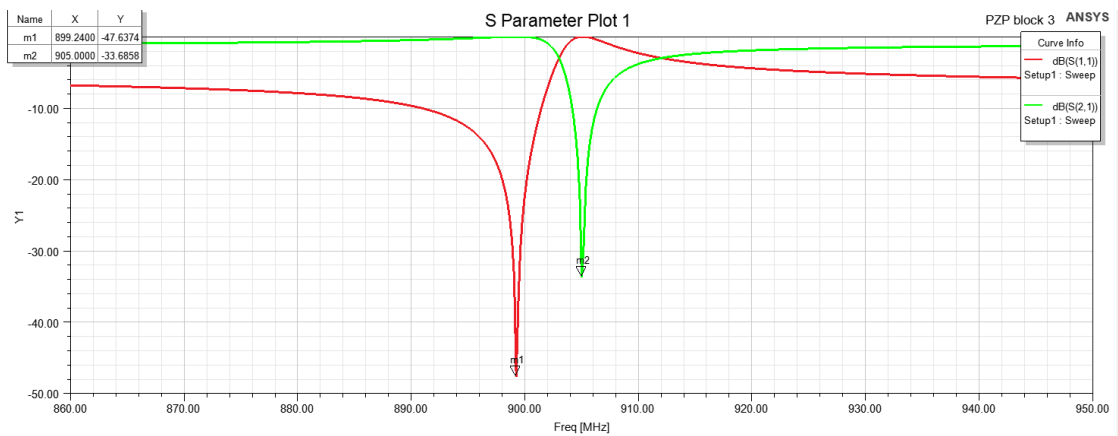


Figure 4.30: Scattering parameters of block 3

4.3 Physical Implementation with Coaxial Technology

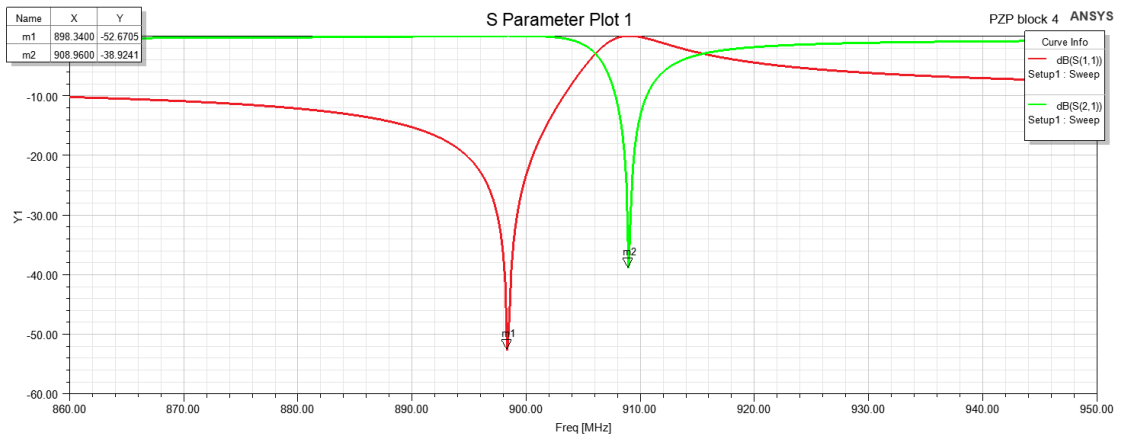


Figure 4.31: Scattering parameters of block 4

To clearly show the interference of tuning on the obtained X_{eq} and B_{nrn} , the detailed results are shown in Tab.4.5:

	Block 1		Block 2		Block 3		Block 4	
	X_{eq}	B_{nrn}	X_{eq}	B_{nrn}	X_{eq}	B_{nrn}	X_{eq}	B_{nrn}
Synthesized result	48.059	-0.565	48.522	-1.171	71.703	-1.096	56.097	-0.758
Before tuning	48.02	-0.576	48.492	-1.17	71.11	-1.08	56.03	-0.761
After tuning	47.9	-0.568	48.34	-1.19	71.07	-1.11	55.99	-0.76

Table 4.5: Comparison of X_{eq} , B_{nrn} of synthesized result, before tuning and after tuning

Additionally, the lengths ϕ_p of the equivalent circuit of the dimensioned blocks are shown in the Tab.4.6:

4.3 Physical Implementation with Coaxial Technology

	Block 1	Block 2	Block 3	Block 4
ϕ_p	0.275°	-0.151°	0.049°	0.174°

Table 4.6: lengths ϕ_p of the equivalent circuit of the dimensioned blocks

4.3.3 Cascading the Blocks with Suitable Length

Until now all the blocks are dimensioned correctly, the only remaining work is to derive the suitable lengths between blocks. Then the filter is obtained by connecting the blocks with transmission lines with suitable lengths.

With the equivalent circuit of PZP block, the final equivalent circuit of cascade-blocks is shown in Fig.4.32:

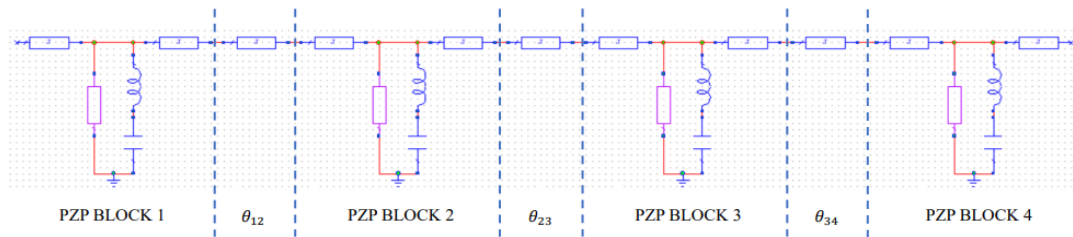


Figure 4.32: Final Equivalent Circuit of Cascade-Blocks

We have already obtained the lengths from the synthesized result, as shown in Tab.4.7:

θ_{12}	θ_{23}	θ_{34}
90°	87.31°	90°

Table 4.7: Computed lengths from the synthesized result

4.3 Physical Implementation with Coaxial Technology

Then we need to transform the electrical lengths into physical lengths. With the tool Wavelength Calculator in HFSS, we could easily compute the wavelength λ with frequency equal to 908MHz ., as shown in Fig.4.33

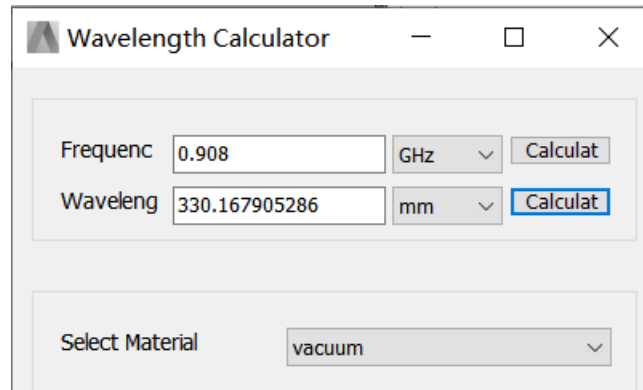


Figure 4.33: Wavelength calculator

Then we transform the electrical lengths θ in the synthesized filter into the lengths l in the equivalent circuit, as shown in Tab.4.7.

$$l = \frac{\lambda\theta}{360^\circ} \quad (4.17)$$

Electrical length	θ_{12} = 90°	θ_{23} = 87.31°	θ_{34} = 90°
Physical length	l_{12} = 82.54198mm	l_{23} = 80.07489mm	l_{34} = 82.54198mm

Table 4.8: Transformation from electrical lengths to physical lengths

It must be observed that the physical length d_{12} , d_{23} and d_{34} is the distance between the reference sections of two adjacent blocks, as shown in Fig.4.34. However, these distances $d_{i,i+1}$ do not coincide with the computed length $l_{i,i+1}$. We have in fact to take into account the loading effects of the PZP blocks represented by the lines $\theta_{p,i}$ in the equivalent circuit.

4.3 Physical Implementation with Coaxial Technology

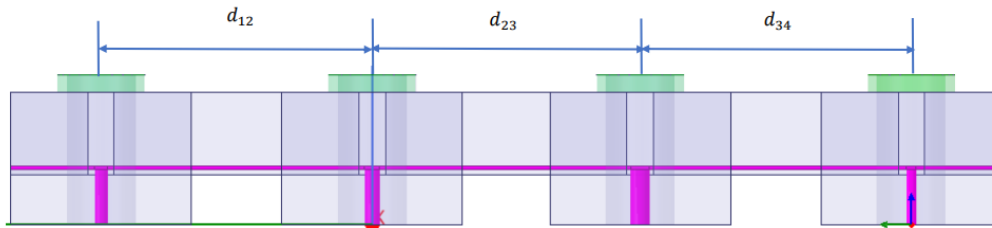


Figure 4.34: Physical model of the final filter

Consequently, the physical lengths between the blocks ($d_{i,i+1}$) are obtained as follows:

$$d_{i,i+1} = l_{i,i+1} - \theta_{p,i}/\beta_0 - \theta_{p,i+1}/\beta_0 \quad (4.18)$$

Then we could derive the distances between the blocks and use them to cascade the blocks, as shown in Tab.4.8:

d_{12}	d_{23}	d_{34}
82.42826mm	80.16844mm	82.33746mm

Table 4.9: Distances between the blocks

However, with these values of lengths, the response of the cascaded blocks (the final filter) is not as satisfying as expected. Actually, a retouch of these lengths is needed. We use a circuit simulator to do this work, as shown in Fig.4.35 and Fig.4.36.

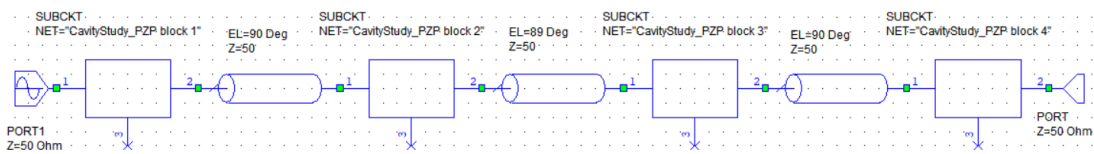


Figure 4.35: Retouch of the connection length in the circuit simulator

AWR

4.3 Physical Implementation with Coaxial Technology

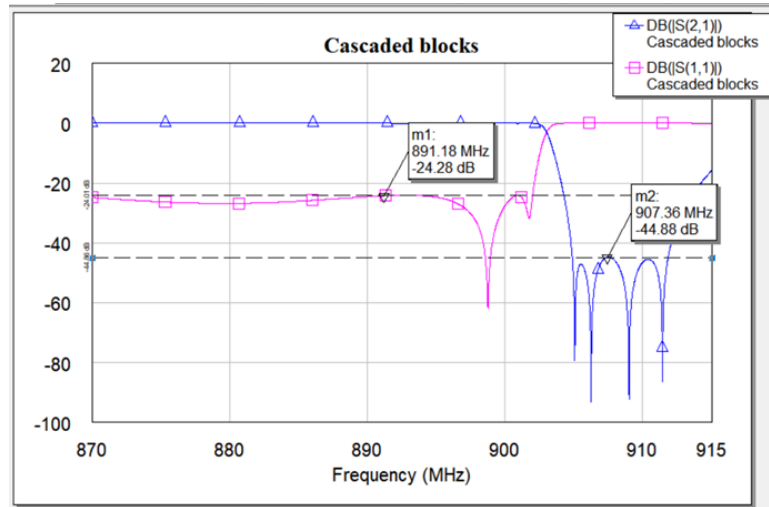


Figure 4.36: Scattering parameters of the filter in the circuit simulator AWR

The final computed distances $d_{i,i+1}$ are shown in Tab.4.9:

d_{12}	d_{23}	d_{34}
82.54198mm	81.5833mm	82.54198mm

Table 4.10: Final computed distances $d_{i,i+1}$

Finally we obtain all the geometrical dimension parameters for the figure, and we compute the scattering parameters of the physical structure with HFSS. The result is compliant with the assigned requirements everywhere and we can say that we have realized our design goal. The final structure is shown in Fig.4.37 and the scattering parameters are shown in Fig.4.38:

4.3 Physical Implementation with Coaxial Technology

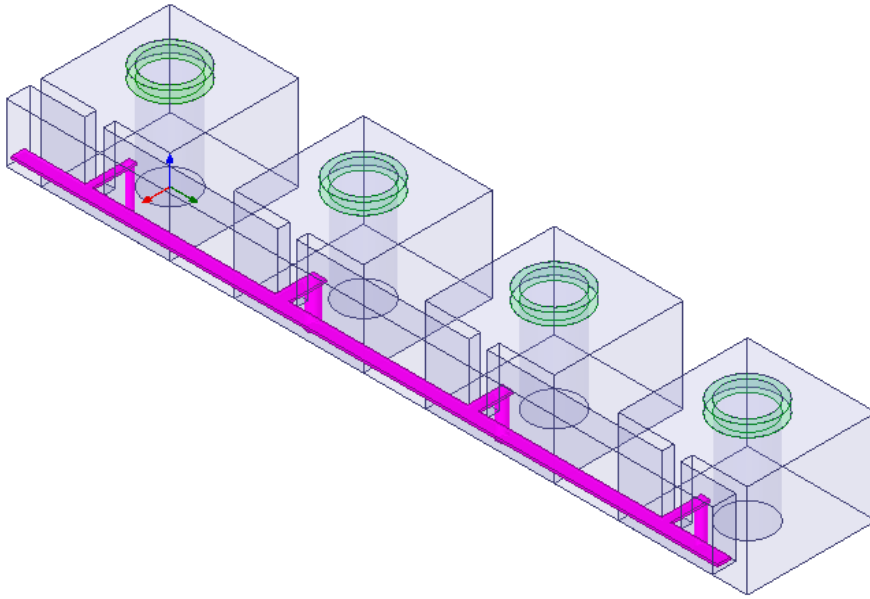


Figure 4.37: Structure of the final filter



Figure 4.38: Scattering parameters of the final filter

Chapter 5

Conclusion and Comments

In this thesis, we have introduced the whole process of the design of an extracted-pole filter in coaxial technology step by step, including the assignment of electrical specification, synthesis of characteristic polynomials, synthesis of low-pass prototype, de-normalization of low-pass prototype and physical implementation of the filter.

Concerning the last point, this thesis introduced a concept called “Divide and Conquer”. Actually we can break the design of the whole filter into several pole-zero pairs (PZP) blocks. Then we try to obtain suitable geometrical dimension for each blocks and finally cascade them with suitable lengths. During this process, the thesis also discusses how to obtain a feasible equivalent circuit for physical implementation.

In this thesis, we apply coaxial technology in the physical implementation. It is performed through coaxial rejection cavities coupled to the boxed stripline, and the loop creates the required negative susceptance of NRN. The final scattering parameters shows that this structure is suitable for the realization of an extracted-pole filter.

5 Conclusion and Comments

Additionally, this thesis introduces a general method suitable for geometrical dimension of a PZP block. Since we could derive the scattering parameters through HFSS simulation, then we could compute X_{eq} , B_{nrn} and transmission zero, which makes to find the geometrical dimensions easier. Firstly we divide the variable used for geometrical into two dimension categories: global parameters and local parameters. Then we could use global parameters to obtain a resonating frequency approximately equal to 900MHz and characteristic impedance equal to 50 Ω . Then next step is to use local parameters to obtain required X_{eq} and B_{nrn} .

In this step, this thesis introduced a general method, which could obtain suitable value of local parameter quickly and correctly. This method helps designer save a lot of time.

However, it is worth mentioning that the solution pair (Rs, s) is obtained based on the intersection of two curves. It is possible that there are no intersections, or the intersection is out of the feasible range of (Rs, s) . Actually the second phenomenon is more common. Fig.5.1 is an example ($X_{eq} = 48.522$, which is equal to the second block in chapter 4, while $B_{nrn} = -1.4$ not -1.171 in the second block)

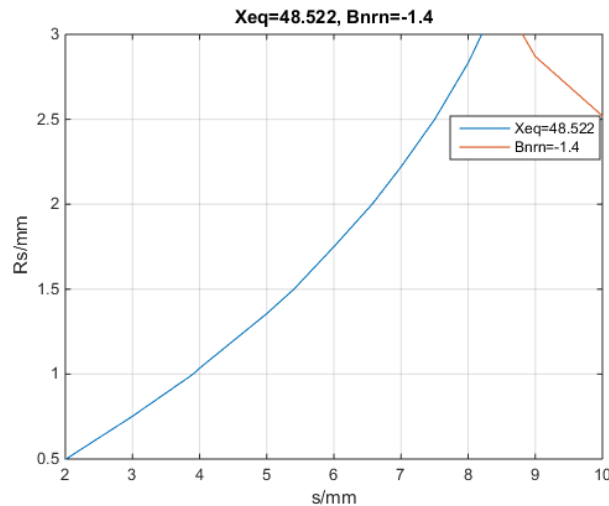


Figure 5.1: $X_{eq} = 48.522$, $B_{nrn} = -1.4$
(block 2 with equal X_{eq} but larger $|B_{nrn}|$)

5 Conclusion and Comments

Actually the intersection is out of the range of the figure, it means that in solution pair (s, R_s) , R_s must be larger than $3mm$. But the gap between the side wall and the strip must be at least as large as half of the strip width, with $A = 8mm$, $R_s = 3mm$, the remaining gap is $1mm$, which is the best condition. If R_s is larger than $3mm$, A must be increased to have enough gap.

In the case that $B_{nrn} = -1.4$, in other words, the required negative susceptance is not quite large. We can use the method above, increase both A and R_s to try to find a feasible solution.

However, when the required susceptance is quite large, the method above could not be suitable since A will be quite large. At the circuit level, it means that the negative susceptance created by the loop is not enough. To increase the obtained negative susceptance for NRN, an additional short-circuit post can be added to obtain the required NRN value, which is shown in Fig.5.2:

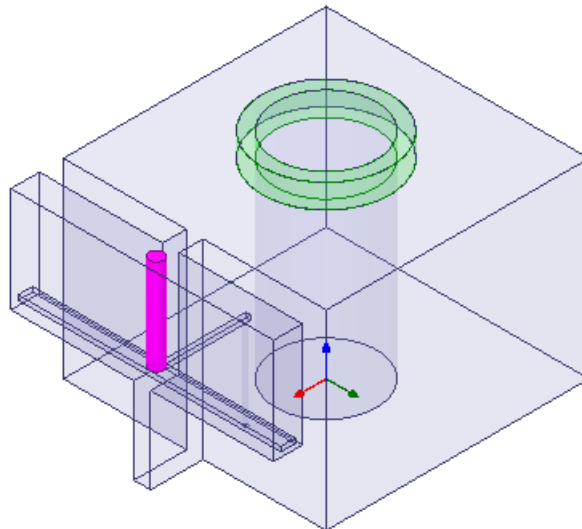


Figure 5.2: Physical implementation of PZP block with addition short-circuited post

5 Conclusion and Comments

This structure will create a much large negative susceptance (become larger with the increase of the radius of NRN), and synthesized filters with large negative susceptance will benefit from this structure.

Bibliography

- [1] R. J. Cameron, C. M. Kudsia, and R. R. Mansour, *Microwave Filters for Communication Systems: Fundamentals, Design and Applications*, 2nd ed., Hoboken, NJ, USA: Wiley, 2018.
- [2] G. Macchiarella "Generalized Coupling Coefficient for Filters With Nonresonant Nodes" in *IEEE Microwave And Wireless Components Letters*, Vol. 18, No. 12, pp. 773-775, Dec. 2008
- [3] S. C. Mejillones, M. Oldoni, S. Moscato, G. Macchiarella, M. D'Amico and G. G. Gentili, "Accurate Synthesis of Extracted-Pole Filters by Topology Transformations," in *IEEE Microwave and Wireless Components Letters*, vol. 31, no. 1, pp. 13-16, Jan. 2021.
- [4] R. J. Cameron, "Advanced coupling matrix synthesis techniques for microwave filters", *IEEE Trans. Microw. Theory Techn.*, vol. 51, no. 1, pp. 1-10, Jan. 2003.
- [5] S. Tamiazzo and G. Macchiarella, "An analytical technique for the synthesis of cascaded N-tuplets cross-coupled resonators microwave filters using matrix rotations", *IEEE Trans. Microw. Theory Techn.*, vol. 53, no. 5, pp. 1693-1698, May 2005.

- [6] G. Macchiarella “Generalized Coupling Coefficient for Filters With Nonresonant Nodes” in IEEE Microwave And Wireless Components Letters, Vol. 18, No. 12, pp. 773-775, Dec. 2008.
- [7] R. J Cameron, “General Coupling Matrix Synthesis Methods for Chebyshev Filtering Functions,” IEEE Transactions On Microwave Theory And Techniques, Vol. 47, No. 4, April 1999.
- [8] S. Amari and U. Rosenberg, “Direct synthesis of a new class of bandstop filters,” in IEEE Transactions on Microwave Theory and Techniques, vol. 52, no. 2, pp. 607–616, Feb. 2004
- [9] M. Oldoni, G. Macchiarella and F. Seyfert, Synthesis and Modelling Techniques for Microwave Filters and Diplexers: Advances in Analytical Methods With Applications to Design and Tuning, Saarbrücken, Germany:Scholars’ Press, Feb. 2014.